Developmental Biology 455 (2019) 458–472

Contents lists available at ScienceDirect

Developmental Biology

journal homepage: www.elsevier.com/locate/developmentalbiology

Original research article

YAP1 is involved in replenishment of granule cell precursors following injury to the neonatal cerebellum

Zhaohui Yang [a,b], Alexandra L. Joyner [a,b,*]

[a] Biochemistry, Cell and Molecular Biology Program, Weill Cornell Graduate School of Medical Sciences, New York, NY, 10065, United States
[b] Developmental Biology Program, Sloan Kettering Institute, New York, NY, 10065, United States

ARTICLE INFO

Keywords:
Hippo signaling
Adaptive reprogramming
Nestin-expressing progenitors
Yes-associated protein
Taz

ABSTRACT

The cerebellum undergoes major rapid growth during the third trimester and early neonatal stage in humans, making it vulnerable to injuries in pre-term babies. Experiments in mice have revealed a remarkable ability of the neonatal cerebellum to recover from injuries around birth. In particular, recovery following irradiation-induced ablation of granule cell precursors (GCPs) involves adaptive reprogramming of Nestin-expressing glial progenitors (NEPs). Sonic hedgehog signaling is required for the initial step in NEP reprogramming; however, the full spectrum of developmental signaling pathways that promote NEP-driven regeneration is not known. Since the growth regulatory Hippo pathway has been implicated in the repair of several tissue types, we tested whether Hippo signaling is involved in regeneration of the cerebellum. Using mouse models, we found that the Hippo pathway transcriptional co-activator YAP1 (Yes-associated protein 1) but not TAZ (transcriptional coactivator with PDZ binding motif, or WWTR1) is required in NEPs for full recovery of cerebellar growth following irradiation one day after birth. Although *Yap1* plays only a minor role during normal development in differentiation of NEPs or GCPs, the size of the cerebellum, and in particular the internal granule cell layer produced by GCPs, is significantly reduced in *Yap1* mutants after irradiation, and the organization of Purkinje cells and Bergmann glial fibers is disrupted. The initial proliferative response of *Yap1* mutant NEPs to irradiation is normal and the cells migrate to the GCP niche, but subsequently there is increased cell death of GCPs and altered migration of granule cells, possibly due to defects in Bergmann glia. Moreover, loss of *Taz* along with *Yap1* in NEPs does not abrogate regeneration or alter development of the cerebellum. Our study provides new insights into the molecular signaling underlying postnatal cerebellar development and regeneration.

1. Introduction

The cerebellum not only has a principal role in motor coordination and balance control, but also is linked to a wide range of higher order cognitive and social functions (Fatemi et al., 2012; Marek et al., 2018; Stoodley et al., 2017; Tsai et al., 2012; Tsai et al., 2018; S. S. Wang, Kloth and Badura, 2014). Development of the cerebellum in both human and mouse is a protracted process, much of which spans from late embryonic to early postnatal stages (Altman and Bayer, 1997; Dobbing and Sands, 1973; Rakic and Sidman, 1970). Therefore, the cerebellum is particularly vulnerable to clinical and environmental insults around birth. Indeed, cerebellar injury is a frequent complication of premature birth and can lead to reduced cerebellar size (Biran et al., 2012; Steggerda et al., 2009) and to long-term neurodevelopmental problems including in motor, cognitive, social and language development (Brossard-Racine et al., 2015; Hortensius et al., 2018; Limperopoulos et al., 2007; Messerschmidt et al., 2008; Wang et al., 2014). Thus, it is crucial to dissect the molecular mechanisms that underlie processes of repair in the neonatal cerebellum.

The mouse cerebellum originates from the anterior hindbrain and undergoes substantial growth in the first two postnatal weeks. Prior to birth (embryonic day (E) 13.5–15.5), the *Atoh1*-expressing granule cell precursors (GCPs) migrate over the surface of the cerebellum. After birth, GCPs rapidly proliferate in the external granule cell layer (EGL) in response to Sonic Hedgehog (SHH) secreted by Purkinje cells (PCs) (Corrales et al., 2006; Lewis et al., 2004; Sillitoe and Joyner, 2007). Until approximately postnatal day (P) 15, post-mitotic GCPs migrate down Bergmann glial fibers and past the Purkinje cell layer (PCL) to populate the internal granule cell layer (IGL) and complete differentiation and maturation (Sillitoe and Joyner, 2007). By following up on an earlier finding in infant rats that the EGL is rapidly reconstituted several days

* Corresponding author. Developmental Biology Program Sloan Kettering Institute, 1275 York Avenue, Box 511, New York, NY, 10065, United States.
E-mail address: joynera@mskcc.org (A.L. Joyner).

https://doi.org/10.1016/j.ydbio.2019.07.018
Received 29 March 2019; Received in revised form 30 July 2019; Accepted 30 July 2019
Available online 31 July 2019

after depletion by irradiation (Altman et al., 1969), we found that the cerebellum of the neonatal mouse is capable of substantial recovery of growth after ablation of most GCPs in the EGL by irradiation at P1 (Wojcinski et al., 2017). Furthermore, PCs are completely replenished when ~50% are killed at P1, in an age-dependent process that involves a rare immature PC population proliferating and producing new PCs (Bayin et al., 2018). Thus, at least two cell types in the cerebellum are effectively replenished when ablated soon after birth, and each involves a distinct cellular process.

The regeneration of GCPs after their depletion is dependent on a proliferative subpopulation of Nestin-expressing progenitors (NEPs), which are derived from the ventricular zone during late-embryogenesis (Buffo and Rossi, 2013; Fleming et al., 2013; Milosevic and Goldman, 2004). There are two main subpopulations of NEPs, one that resides in the PCL and gives rise to astrocytes and Bergmann glia and the other in the white matter (WM) produces interneurons and astrocytes (Cerrato et al., 2018; Fleming et al., 2013; Li et al., 2013; Parmigiani et al., 2015; Wojcinski et al., 2017). Furthermore, both populations rely on SHH for their proliferation. When GCPs in the EGL are depleted genetically or by irradiation at P1, NEPs in the PCL sense the injury and respond by increasing cell proliferation and then migrating into the EGL where they switch their fate to GCPs and produce granule cells that contribute to the IGL (Andreotti et al., 2018; Jaeger and Jessberger, 2017; Wojcinski et al., 2017; Wojcinski et al., 2019). At the same time, NEPs in the WM transiently reduce their production of interneurons and astrocytes. Although SHH signaling is required for NEPs to replenish the injured EGL (Wojcinski et al., 2017), the full molecular repertoire underlying the regenerative capacity of NEPs remains to be determined.

The Hippo signaling pathway is a key regulator of size control of many organs (Halder and Johnson, 2011; Pan, 2010) through regulating cell proliferation and cell survival (Ardestani and Maedler, 2018; Emoto, 2011; Ikeda and Sadoshima, 2016; M. Lee, Goraya, Kim and Cho, 2018; Udan et al., 2003; Wu et al., 2003). In mammals, upon activation of a conserved kinase cascade consisting of the serine/threonine kinases MST1/2 (mammalian Ste2-like kinases) and LATS1/2 (large tumor suppressor kinase 1/2), the transcriptional cofactors Yes-associated protein 1 (YAP1) and transcriptional coactivator with PDZ binding motif (TAZ, also called WWTR1, for WW-domain containing transcription regulator 1) are phosphorylated, sequestered by 14-3-3 in the cytoplasm, and targeted for degradation in a ubiquitin-proteasome-dependent manner (Callus et al., 2006; Chan et al., 2005; Y. Liu and Deng, 2019; Nguyen and Kugler, 2018; Wu et al., 2003; Zhao et al., 2010). Conversely, in the absence of Hippo signaling, dephosphorylated YAP1 and TAZ translocate into the nucleus and form complexes with the TEAD/TEF family of transcription factors to activate downstream transcriptional programs that include promotion of cell proliferation and organ growth (K. Wang, Degerny, Xu and Yang, 2009). Although YAP1 is known to regulate the renewal of many tissue types after injury, including liver, incisors, and the colonic epithelium (Hu et al., 2017; Lu et al., 2018; Yui et al., 2018), the role of YAP1/TAZ in mammalian brain development and regeneration remains poorly studied. Conditional genetic ablation of *Yap1* (referred to as *Yap*) in radial glial progenitor cells (using *Nestin-Cre*) was found to cause hydrocephalus and a subtle defect in the proliferation of cortical neural progenitors, but no major anatomical changes in the brain (Park et al., 2016). On the other hand, inactivation of LATS1/2 from the same (Nestin+) neural progenitor population during brain development in mouse was shown to result in YAP/TAZ-driven global hyper-transcription with upregulation of many target genes related to cell growth and proliferation (Lavado et al., 2018). The gene expression changes are thought to inhibit the differentiation of neural progenitors and promote transient over-proliferation of neural progenitors. In an *ex vivo* model, it was shown that *Yap* over-expression increases the proliferation of cultured GCPs, while shRNA knockdown of *Yap* decreases proliferation (Fernandez et al., 2009). Moreover, *Yap* over-expression was reported to protect cultured GCPs from irradiation-induced damage by sustaining their proliferation and survival (Fernandez et al., 2012). However, the potential function of YAP/TAZ in development and regeneration of the neonatal cerebellum has not been tested *in vivo*.

Here we utilized genetic deletion of *Yap* and/or *Taz* in mice and revealed an essential role for YAP in mammalian cerebellar regeneration following irradiation, but only a minor role in inhibiting differentiation during cerebellar development. Loss of *Yap* at P0 from NEPs disrupted restoration of cerebellar size following irradiation with pronounced reduction in the IGL and disorganization of PCs and Bergmann glial fibers. The poor recovery of the cerebellum was associated with elevated death of the NEPs in the PCL one day after irradiation and later death of GCPs in the EGL, and defective migration of the granule cells into the IGL potentially due to a defect in Burgmann glia. In contrast, loss of *Yap* at P0 in NEPs or GCPs in conditional knockout (cKO) mice resulted in only mild enhancement of differentiation of NEPs and GCPs and no alteration of the size or morphology of the adult cerebellum. Surprisingly, loss of *Taz* in addition to *Yap* at P0 in NEPs did not alter cerebellar development or reduce the recovery of the IGL after irradiation. Our study identifies Hippo signaling as a key molecular signaling pathway underlying the late stage of regeneration of the postnatal EGL following injury. Our discovery also raises the possibility that inhibiting Hippo signaling could reduce cerebellar hypoplasia after injury through enhancing recovery.

2. Materials and methods

2.1. Mice

The following mouse lines were used: *Nes-CFP* (Mignone et al., 2004), *Atoh1-GFP* (Chen et al., 2002), *Nestin-FlpoER* (Wojcinski et al., 2017), *Atoh1-FlpoER* (Wojcinski et al., 2019), *Rosa26*$^{MASTR(frt\text{-}STOP\text{-}frt\text{-}GFPcre)}$ (Lao et al., 2012), *Yap*$^{flox/flox}$ and *Taz*$^{flox/flox}$ (Reginensi et al., 2013), and *Atoh1-Cre* (Matei et al., 2005). Tamoxifen (Sigma, T5648) was dissolved in corn oil at 20 mg/mL and a single dose of 200 μg/g was administered to P0 animals by subcutaneous injection. Mouse husbandry and all experiments were performed in accordance with MSKCC IACUC-approved protocols.

2.2. Irradiation

P1 mice were anesthetized by hypothermia and received a single dose of 4 Gy irradiation in an X-RAD 225Cx (Precision X-ray) Microirradiator in the MSKCC Small-Animal Imaging Core Facility. A 5-mm diameter collimator was used to target the cerebellum from the left side of the animal.

2.3. Tissue processing

Animals younger than P4 were sacrificed and then brains were dissected and fixed in 4% paraformaldehyde overnight at 4°C. Animals P4-30 were anesthetized and transcardially perfused with PBS followed by chilled 4% paraformaldehyde. Brains were dissected and post-fixed overnight and cryoprotected in 30% sucrose before freezing in Cryo-OCT. Frozen brains were cryosectioned sagittally at 12 μm. Midline cerebellar sections were used for all analyses.

2.4. Immunofluorescent staining

Cryosections were stained overnight at 4 °C with the following primary antibodies: mouse anti-YAP (Abcam, AB56701), rabbit anti-TAZ (Santa Cruz, sc-48805), rat anti-GFP (1:1000; Nacalai Tesque; 0440484), mouse anti-NeuN (Millipore, MAB377), rabbit anti-Calbindin D-28K (Swant, CB38), rabbit anti-GFAP (Dako, Z0334), rabbit anti-S100β (Dako, Z0311), rabbit anti-PAX2 (Invitrogen, 71600), goat anti-SOX2 (R&D System, AF2018), rabbit anti-PAX6 (Millipore, AB2237), and rabbit anti-cleaved Caspase3 (Cell Signaling Technology, 9664S). Secondary antibodies for double labeling were donkey anti-species conjugated with Alexa Fluor 488 or 555 (1:1000; Molecular Probes). Nuclei

were counterstained with Hoechst 33258 (Invitrogen, H3569).

2.5. Microscopy

Images were collected either on a DM6000 Leica microscope using Zen software (Zeiss), or a NanoZoomer 2.0 HT slide scanner (Hamamatsu Photonics) using NDP. scan software. All images were taken with 20X objectives and processed using NDP. view2 or Photoshop softwares.

2.6. Flow Cytometry

Cerebella of *Atoh1-GFP* and *Nestin-CFP* mice were dissected out under a dissection microscope. Tissues were digested by Trypsin/DNase, and then subject to FACS (fluorescence activated cell sorting) to isolate GFP+ or CFP+ cells.

2.7. RT-qPCR

RNA was isolated from FACS-isolated GFP+ cells from P4 *Atoh1-GFP* mice and FACS-isolated CFP+ cells from *Nestin-CFP* mice using a miRNeasyMicro Kit (Qiagen) according to the manufacturer's protocol. cDNA was prepared using iScript cDNA synthesis kit (Bio-Rad). RT-qPCR was performed using PowerUp Sybr Green Master Mix (Applied Biosystems). Fold changes in expression were calculated using the ΔΔCt method. The *Gapdh* gene was used to normalize the results. The following primer pairs were used: *Yap* forward 5′- ACCCTCGTTTTGCCATGAAC-3′, *Yap* reverse 5′- TGTGCTGGGATTGATATTCCGTA-3′, *Taz* forward 5′- CATGGCGGAAAAAGATCCTCC-3′, *Taz* reverse 5′- GTCGGTCACGTCATAGGACTG-3′, *Gapdh* forward 5′- CCAAGGTGTCCGTCGTGGATCT-3′, and *Gapdh* reverse 5′- GTTGAAGTCGCAGGAGACAACC-3'.

2.8. Quantification and statistical analysis

ImageJ software was used to measure the area (mm^2) of the cerebellum on sections near the midline. Cell counts from IF staining were obtained using Stereo Investigator Software. Four sections per animal for the TUNEL quantifications at P12 cerebella, or three sections per animal for all the other quantifications were analyzed on at least three animals. Statistical analyses were performed using Prism software (GraphPad) and significance was determined at $P < 0.05$. All statistical analyses were two-tailed. For two-group comparisons with equal variance as determined by the F-test, an unpaired Student's *t*-test was used. For comparisons among four independent groups with equal variance, an unpaired one-way ANOVA was used. For comparisons between groups that are split with two independent variables, an unpaired two-way ANOVA was used. P values and degrees of freedom are given in the figures and legends. Data are presented as mean ± S.D. (standard deviation). No statistical methods were used to predetermine the sample size, but our sample sizes are similar to those generally employed in the field. No randomization was used. Data collection and analysis were not performed blind to the conditions of the experiments.

2.9. EdU (5-ethynyl-2′-deoxyuridine) injection and staining

For assessing cell proliferation, EdU (Invitrogen, E10187) was given at 100 mg/g by i. p. injection 1 h before euthanasia. Click-it EdU assay with Sulfo-Cyanine5 azide (Lumiprobe corporation, A3330) was used according to the protocol of the manufacturer.

2.10. TUNEL staining

For TUNEL staining, slides were permeabilized with 0.5% TritonX-100, pre-incubated with Tdt buffer (30 mM Tris·HCl, 140 mM sodium cacodylate and 1 mM $CoCl_2$) for 15 min at room temperature, and incubated for I h at 37 °C in TUNEL reaction solution containing Terminal Transferase (Roche, 03333574001) and Digoxigenin-11-dUTP (Sigma-Aldrich, 11093088910). Slides were then incubated with anti-digoxigenin-rhodamine (Sigma-Aldrich, 11207750910) for 1 h.

3. Results

3.1. YAP and TAZ expression are enriched in NEPs in the neonatal cerebellum

As a first step in studying the functions of YAP and TAZ in the developing and regenerating cerebellum, we characterized the expression of the proteins in *Nestin-CFP* reporter mice using immunofluorescence (IF). It was previously reported that YAP is expressed in GCPs (Fernandez et al., 2009), but expression in NEPs was not addressed. In the cerebella of normal P4 mice, a low level of nuclear YAP was detected in some NEPs (CFP+ cells) whereas in GCPs in the EGL little or no YAP was detected (Fig. 1A,A′,A″). Since NEPs contribute to regeneration of the irradiated (IR) mouse cerebellum, we asked whether YAP expression changes in NEPs during their adaptive reprogramming following irradiation of the cerebellum. When the cerebella of *Nestin-CFP* transgenic mice were irradiated at P1 (IR mice) and analyzed at P4, nuclear YAP was detected mainly in NEPs (CFP+ cells) with little expression in GCPs (Fig. 1B,B′,B″). Of possible significance, in IR mice most of the CFP+ NEPs in the EGL showed nuclear expression of YAP (Fig. 1B,B′,B″), indicating that YAP could play a role in the adaptive reprogramming response of NEPs to EGL ablation. Nuclear located TAZ expression was more obvious than YAP in NEPs of Non-IR and IR cerebella, with similar expression in the two conditions. TAZ was also present in most NEPs in the EGL of IR mice and not detected in GCPs (Fig. 1C-D,C′-D′,C″-D″).

To confirm that *Yap* and *Taz* are expressed at higher levels in NEPs than GCPs, we carried out quantitative RT-PCR (RT-qPCR) of mRNA from FACS-sorted Nestin-CFP+ NEPs and Atoh1-GFP+ GCPs from P4 IR and Non-IR transgenic mice. Indeed, *Yap* and *Taz* mRNA were significantly lower in GCPs than in NEPs of Non-IR and IR mice, and there were no significant changes after irradiation (Fig. 1E and F). Consistent with the antibody staining and RT-qPCR results, analysis of RNA-seq data from Nestin-CFP+ NEPs isolated by FACS from P5 IR and Non-IR mice (Wojcinski et al., 2017) showed that *Yap* and *Taz* transcripts were present in NEPs, with no significant changes after irradiation and a lower number of reads for *Taz* (Table S1). The transcripts for *Tead1* and *Tead2* were abundant while *Tead3* was minimal (Table S1), indicating that TEAD1/2 are the main binding partners for YAP/TAZ in neonatal NEPs. The Hippo target gene *Birc5* was present and appeared to be slightly upregulated in IR NEPs, but a second target gene *Ctgf* had little expression (Table S1). Together, these data demonstrate that the cerebellar cell type that predominantly expresses *Yap* and *Taz* is NEPs, and thus YAP and TAZ could play a role in the regeneration of the EGL by NEPs following irradiation.

3.2. Loss of Yap in the NEP lineage hampers postnatal cerebellar regeneration

Given the potential role of YAP in NEPs for cerebellar regeneration, we determined whether *Yap* is required for injury-induced regeneration of the cerebellum by mutating *Yap* specifically in NEPs at P0 using a mosaic mutant analysis approach (MASTR, Mosaic mutant Analysis with Spatial and Temporal control of Recombination) (Lao et al., 2012; Wojcinski et al., 2017) (Fig. 2A). An inducible FLP site-specific recombinase expressed from a *Nestin* transgene was used to induce sustained expression of a protein fusion between GFP and CRE (referred to as GFPcre) following injection of tamoxifen (Tm), which then induces recombination of a *Yap* floxed allele (Reginensi et al., 2013), resulting in visualization of the mutant cells and their descendants based on GFP expression (Fig. 2A). Tm was administered to *Nes-FlpoER/+;R26*$^{FSF\text{-}GFPcre/+}$*;Yap*$^{flox/flox}$ mice (*Nes-mYap* cKOs) and controls (*Nes-FlpoER/+;Yap*$^{flox/flox}$, or *R26*$^{FSF\text{-}GFPcre/+}$*;Yap*$^{flox/flox}$, or *Yap*$^{flox/flox}$) at P0, X-ray irradiation was conducted at P1, and the size of cerebellum was measured at P30 (Fig. 2B). Notably, *Nes-mYap* cKOs showed a reduction in cerebellar size

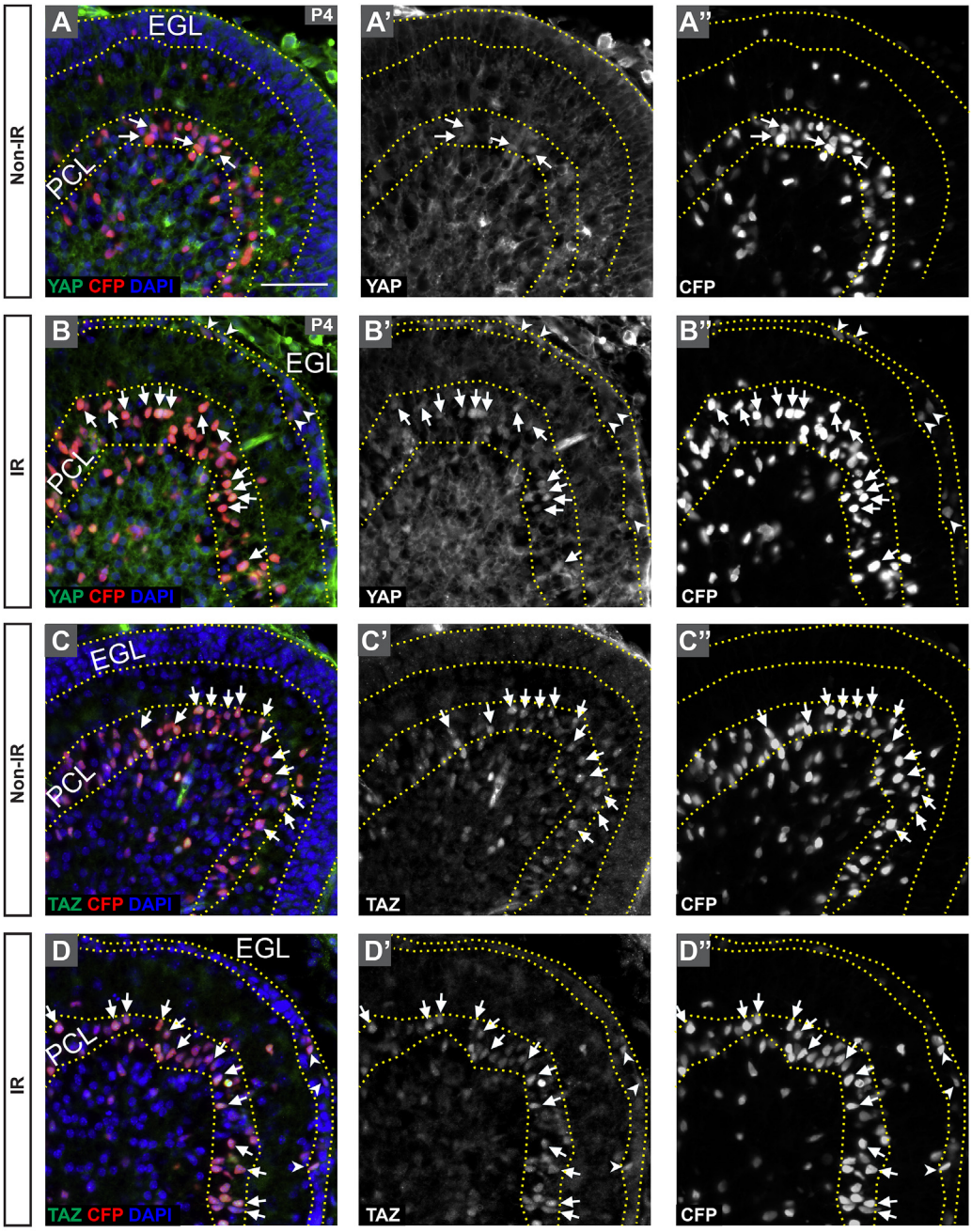

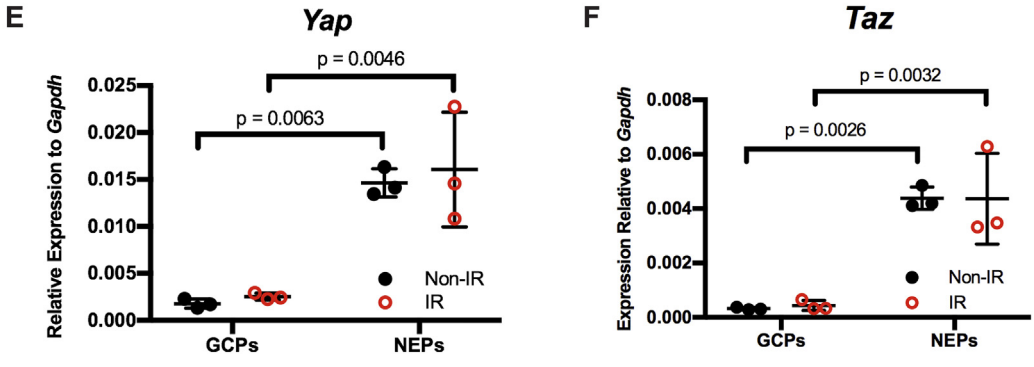

Fig. 1. Nuclear YAP and TAZ are mainly detected in NEPs in the postnatal CB. (A-D) Immunofluorescence (IF) detection of YAP (A-B) and TAZ (C-D), co-stained for CFP and DAPI, on midsagittal sections of cerebella from Non-IR and IR *Nestin-CFP* reporter mice at P4. Arrows and arrowheads indicate *Nestin* (CFP) positive cells in the Purkinje cell layer (PCL) or EGL, respectively that also have nuclear YAP or TAZ. Yellow dotted lines indicate the EGL and PCL. Scale bar, 50 μm. (E-F) RT-qPCR analysis of the mRNA expression of *Yap* (E) and *Taz* (F) relative to *Gapdh* in FACS isolated NEPs (Nestin-CFP+) and GCPs (Atoh1-GFP+) from Non-IR and IR mice at P4. Data are presented as mean ± S.D., and statistical analysis by two-way ANOVA. Each data point represents one animal.

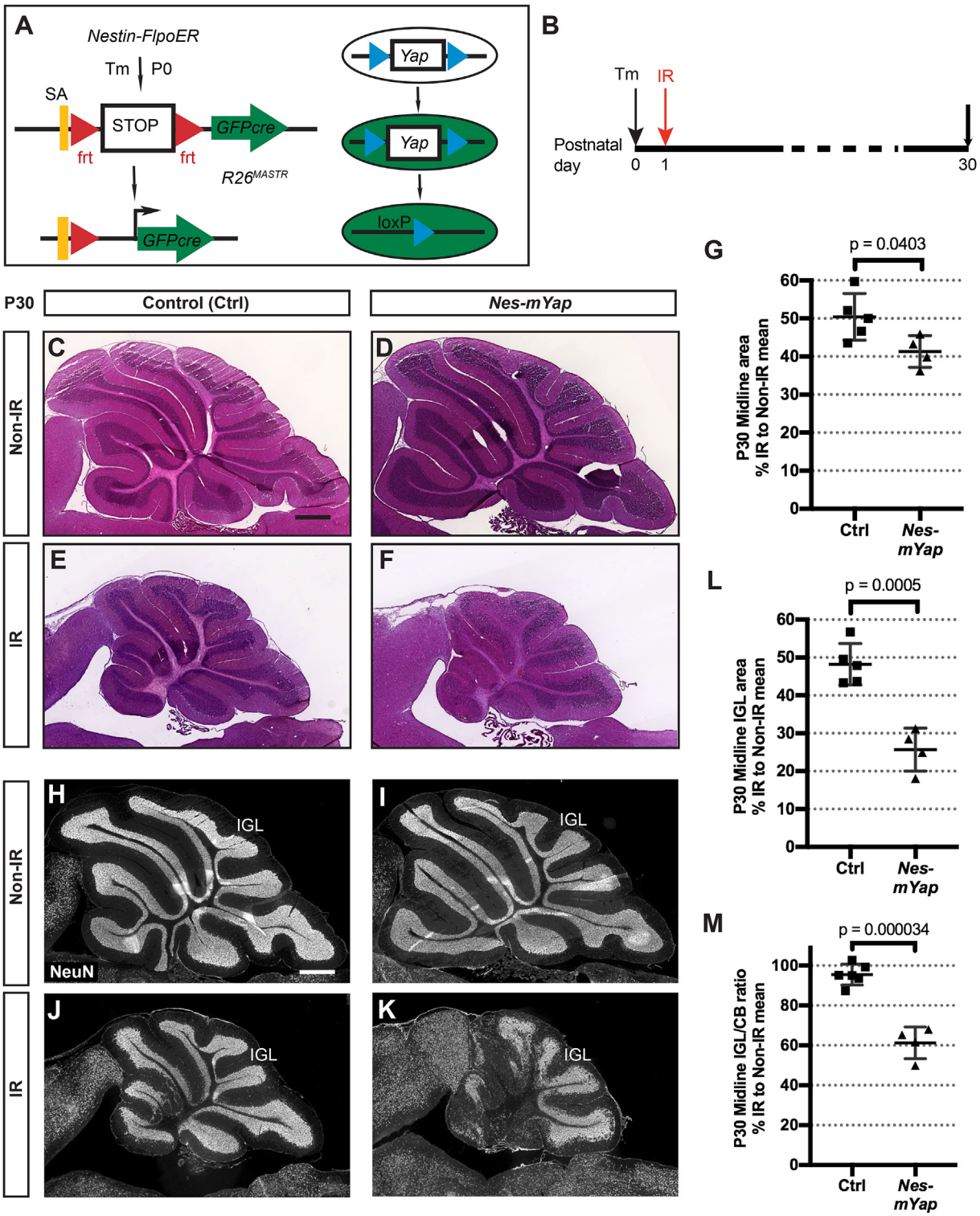

Fig. 2. Mutation of *Yap* in the NEP lineage hampers postnatal cerebellar regeneration. (A) Schematic of the MASTR mosaic mutant technique. (B) Schematic showing experimental design. (C-F) H&E staining of midsagittal sections of the cerebella from Non-IR and IR *Nes-mYap* cKO (Non-IR, n = 6; IR, n = 4) and control mice (Non-IR, n = 4; IR, n = 5) at P30. Scale bar, 500 μm. (G) Graph of the areas of midline sections of the cerebella of IR mice as a percentage of Non-IR animals of the same genotype. (H-K) IF detection of NeuN on midsagittal sections of the cerebella from Non-IR and IR *Nes-mYap* cKOs and controls at P30. Scale bar, 500 μm. (L-M) Graphs of the IGL areas (L) and IGL/cerebellum ratios (M) of midline cerebellar sections of IR *Nes-mYap* cKOs as a percentage of Non-IR mice of the same genotype (Non-IR, n = 6; IR, n = 4) and controls (Non-IR, n = 4; IR, n = 5) at P30. Data are presented as mean ± S.D., and statistical analysis by unpaired *t*-test. Each data point represents one animal and is calculated as the value for each IR mouse (average of 3 sections) divided by the mean for all the Non-IR mice of the same genotype, X 100.

after irradiation compared to IR controls (Fig. 2E and F; Fig. 2S1A). The sizes of the cerebella (area at the midline) of IR mutants were reduced to 41.3 ± 2.10% of Non-IR mutants compared to 50.4 ± 2.75% for IR controls compared to Non-IR controls (Fig. 2G). Even more prominent was a significant reduction in the area of the IGL and ratio of IGL/cerebellum area in *Nes-mYap* cKOs compared to controls following irradiation (Fig. 2H-M; Figs. 2S1B and C). The reduced recovery of the IGL in mutants was most pronounced in lobules 1–5 and 10 (Fig. 2H-K; Figs. 2S1A–C). Furthermore, as is seen in mutant mice with a depleted IGL (Corrales et al., 2006; Corrales et al., 2004), the Calbindin + PCs failed to form a single cell layer in the *Nes-mYap* cKOs; instead, the individual PCs were more disorganized than in controls and dispersed throughout the entire WM-IGL-ML layers (Figs. 2S1D–G,D′-G′). The GFAP+ Bergmann glial fibers also appeared more disorganized in the *Nes-mYap* cKO cerebella (Figs. 2S1H–K, H′-K′). Curiously, the disorganization of the PCs and Bergmann glia in *Nes-mYap* cKO cerebella was more extensive in lobules 1–5 and lobule 10, with lobule 9 being most similar to irradiated controls (Fig. 2S2). Surprisingly, when the areas of the cerebella and IGLs were measured at P12 and P16, we found that IR *Nes-mYap* cKOs and controls had similar IGL/cerebellum ratios at P12 but a significant reduction at P16 (Fig. 2S3). Together, these data indicate a crucial role of YAP in the NEP lineage at a late stage in the recovery of postnatal cerebellar growth after irradiation-induced injury to the EGL.

3.3. Loss of Yap in NEPs results in an increase in cell death one day following irradiation at P1

Since over-expression of YAP in GCPs was shown to protect that cells from irradiation-induced cell death in culture (Fernandez et al., 2012), we examined whether YAP plays a role in maintaining the survival of NEPs in the PCL following irradiation. As expected, cell death (TUNEL+ particles) was minimal in the cerebella of P2 Non-IR *Nes-mYap* cKOs and controls given Tm at P0, and was prominent in the EGL of P2 IR mice (Fig. 3A-E). Interestingly, following irradiation *Nes-mYap* cKOs showed a 1.6-fold increase in the density of TUNEL+ particles within the PCL compared to controls (Fig. 3D,E,F). Since NEPs are the main proliferative cell type in the PCL, this result indicates that YAP protects NEPs from cell death following irradiation. Double labeling for TUNEL or cleaved Caspase3 (CC3) and GFP in *Nes-mYap* cKOs detected only rare TUNEL/GFP double positive cells (~5% of TUNEL+) and a higher percentage of CC3/GFP double positive cells (~15%) (Fig. 3S1). A similar or slightly lower percentage of TUNEL+ or CC3+ cells were labeled with GFP in *Nes-FlpoER/+;R26*$^{FSF\text{-}GFPcre/+}$ (*Nes-m*) wild type IR and Non-IR controls (Fig. 3S1). The low double labeling of GFP and CC3 or TUNEL likely is because GFP degrades rapidly after cell death is initiated. It is therefore not clear whether the cell death is specific to NEPs.

3.4. YAP is dispensable for the migration of NEPs into the EGL following irradiation-induced injury at P1

Given that the area of the IR cerebella of *Nes-mYap* cKOs at P12 was similar to IR controls, we examined whether NEPs are able to migrate into the EGL after irradiation when *Yap* is mutant. The distribution of GFP+ cells derived from NEPs labeled at P0 (and also mutated for *Yap* in *Nes-mYap* cKOs) in the different layers of Lobule 4/5 was quantified in both *Nes-mYap* cKOs and controls (*Nes-m*) at P8 (Fig. 3A). Consistent with the initial recovery of cerebellar area in *Nes-mYap* cKOs compared to IR controls, both the number and the percentage of GFP+ cells in the EGL of IR mice was similar between the two genotypes and much greater than in Non-IR mice (Fig. 3G-L). In addition, the numbers and percentages of NEPs in the molecular layer (ML) and IGL + WM were similar between the two genotypes after irradiation (Fig. 3S2). These results indicate that there is no cell autonomous requirement for YAP in NEPs for their migration from the PCL into the EGL.

3.5. YAP regulates differentiation of NEPs during normal cerebellum development, and the requirement is over-ridden following irradiation

We next examined whether *Yap* is required for the differentiation of NEPs during development of the cerebellum, by determining the distribution within the layers of the cerebellum of the descendants of NEPs labeled at P0 and analyzed at P8. Quantification of the GFPcre+ NEP-derived cells in lobule 4/5 of P8 cerebella demonstrated a significant increase in the number of GFP+ cells in the ML normalized to the area of the lobule analyzed, as well as the percentage of cells in the ML in *Nes-mYap* cKOs compared to *Nes-m* controls (Fig. 4A-E; Figs. 4S1A and B), but no significant change in the total number of mutant cells present at P8 (Fig. 4C; Figs. 4S1A and B). There was a concomitant decrease in the percentage of cells in the IGL + WM layers, but not the total number of cells in the IGL + WM layers, indicating that the significant change in *Nes-mYap* cKOs is an increase in the production of NEP-derived cells that populate the ML (Fig. 4E; Figs. 4S1A and B). Consistent with the GFP+ cells in the ML being the expected interneurons produced by WM-NEPs, there was also a significant increase in the number of cells in the ML that expressed PAX2, a marker of differentiating interneurons (Fig. 2F). The number of PAX2+ cells in the IGL + WM also was increased, but not significantly, indicating that in the absence of *Yap* WM NEPs increase their production of interneurons that migrate to the ML (Fig. 4G; Figs. 4S1C and D). Quantification of S100β+ astrocytes and Bergmann glia among the GFP+ populations in lobule 4/5 revealed an increase in the number of S100β+ cells in the PCL (Bergmann glia), but not S100β+ (astrocytes) in the IGL + WM (Fig. 4H; Figs. 4S1E and F). These data reveal that YAP normally plays a role in attenuating production of interneurons and Bergmann glia.

Given that we did not observe a change in the distribution of *Yap* mutant GFP+ cells in the layers of the P8 cerebellum after irradiation, we next examined whether loss of YAP in NEPs alters their differentiation into interneurons (PAX2+) and astrocytes (S100β+) during irradiation-induced recovery of the cerebellum. No difference was observed in the number or percentage of PAX2+ cells in a specific layer (Figs. 4S2A and B), and there was no difference in the production of S100β+ astrocytes between *Yap* mutant and control mice after irradiation (Figs. 4S2C and D). These results indicate that the requirement for YAP in differentiation of NEPs is over-ridden when the EGL of the cerebellum is injured.

3.6. Loss of YAP results in an increase in cell death in the EGL and a defect in granule cell migration at P12 following irradiation-induced injury at P1

We next analyzed the cerebellum at P12, when the EGL is normally diminishing due to increased production of granule neurons. Quantification of the area and the thickness of the EGL showed no difference between IR *Nes-mYap* cKOs and controls, or in cerebellar IGL area (Fig. 5S1). Given the reduction in the size of the IGL in IR mutants compared to IR controls at P30, we asked whether YAP plays a role in cell survival or migration of granule cells. Strikingly, TUNEL staining in the EGL showed a significant increase in the density of TUNEL+ particles within the EGL (number of TUNEL+ particles per 0.1mm^2) of *Nes-mYap* cKOs compared to controls after irradiation (Fig. 5A-F). In contrast, the density of TUNEL+ particles within the EGL at P8 was not different between controls and mutants (Fig. 5S2), consistent with the similar distributions and numbers of GFP+ cells between the cell layers in the two genotypes at P8. Furthermore, we examined PAX6 staining in the ML to determine whether there was a change in migration of granule cells from the EGL to the IGL, and found a higher density of PAX6+ cells in the ML in lobule 4/5 but not lobule 9 of *Nes-mYap* mutants compared to controls specifically after irradiation (Fig. 5G; Fig. 5S3). Since only rare PAX6+ cells in the ML were GFP+, one possibility is that there is a defect in the *Yap* mutant Bergmann glia that reduces migration of all granule cells (mutant and wild type) (Figs. 2S1H–K). Together, these results indicate that YAP is required for GCPs to maintain cell survival in the EGL and for granule cells to migrate along Bergmann glia through the ML into the IGL

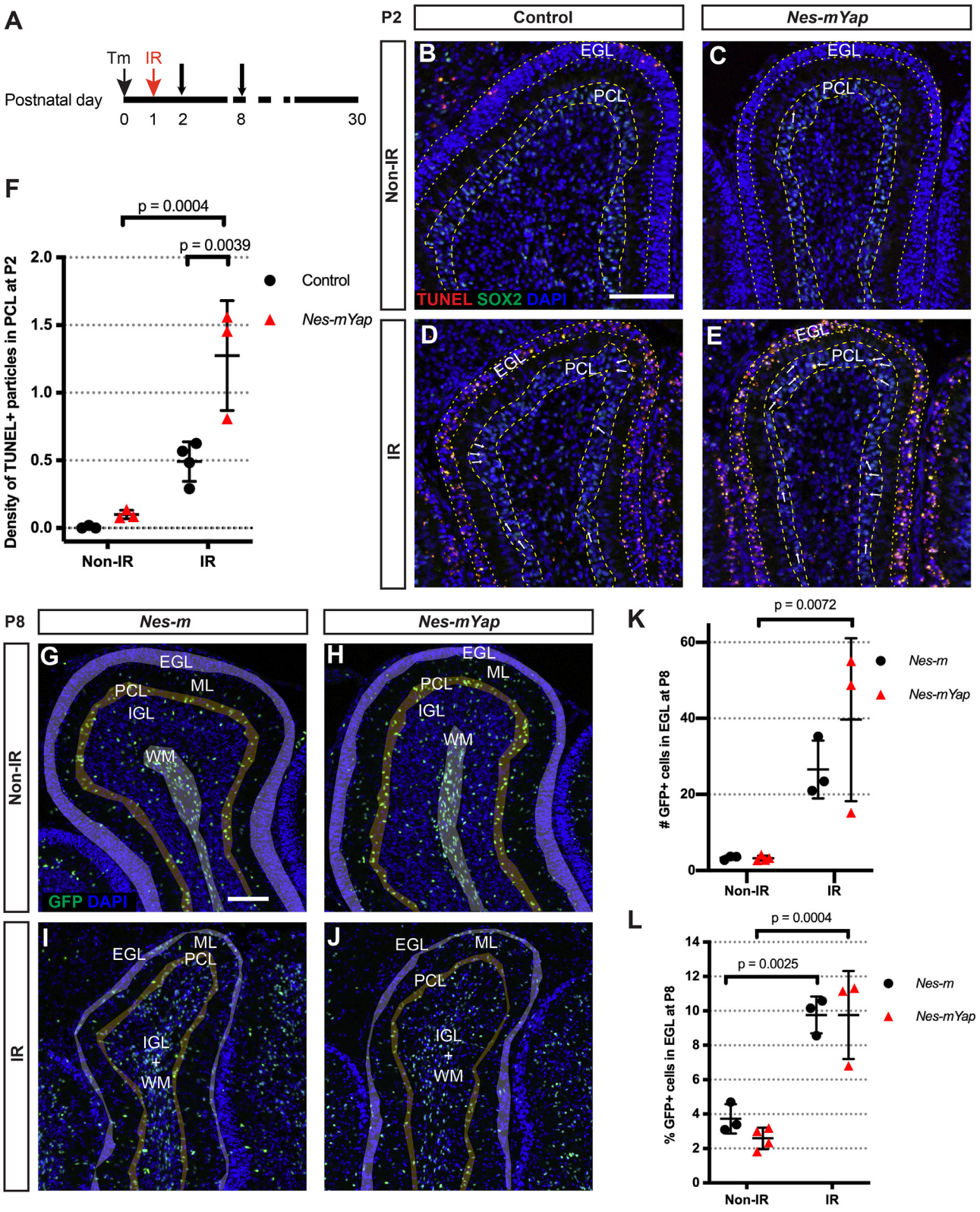

Fig. 3. Deletion of *Yap* in NEPs at P0 results in an increase in cell death in the PCL after irradiation-induced injury at P1. in NEPs at P0 results in an increase in cell death in the PCL after irradiation-induced injury at P1. (A) Schematic showing experimental design. (B-E) Representative images from lobule 4/5 showing IF staining for TUNEL, SOX2, and DAPI on midsagittal sections from IR and Non-IR *Nes-mYap* cKOs and controls one day after IR at P1. Grey shadow highlights the PCL of the lobule. Arrows indicate TUNEL+ particles in the PCL. Scale bar, 100 μm. (F) Graph of the densities of TUNEL+ particles in the PCL of the midline cerebella from IR and Non-IR *Nes-mYap* cKOs (Non-IR, n = 3; IR, n = 3) and controls (Non-IR, n = 3; IR, n = 3) at P2. (G-J) Representative images from lobule 4/5 showing IF staining of GFP and DAPI on midsagittal cerebellar sections from IR and Non-IR *Nes-m* controls and *Nes-mYap* cKOs at P8. Grey shadow highlights the EGL of the lobule. Scale bar, 100 μm. (K-L) Graphs of the numbers of GFP+ cells normalized to total area measured in the EGL (K) and the percentages of GFP+ cells in the EGL among the total number of GFP+ cells (L) from *Nes-m* controls (Non-IR, n = 3; IR, n = 3) and *Nes-mYap* cKOs (Non-IR, n = 4; IR, n = 3) at P8. Data are presented as mean ± S.D., and statistical analysis by two-way ANOVA. Each data point represents one animal.

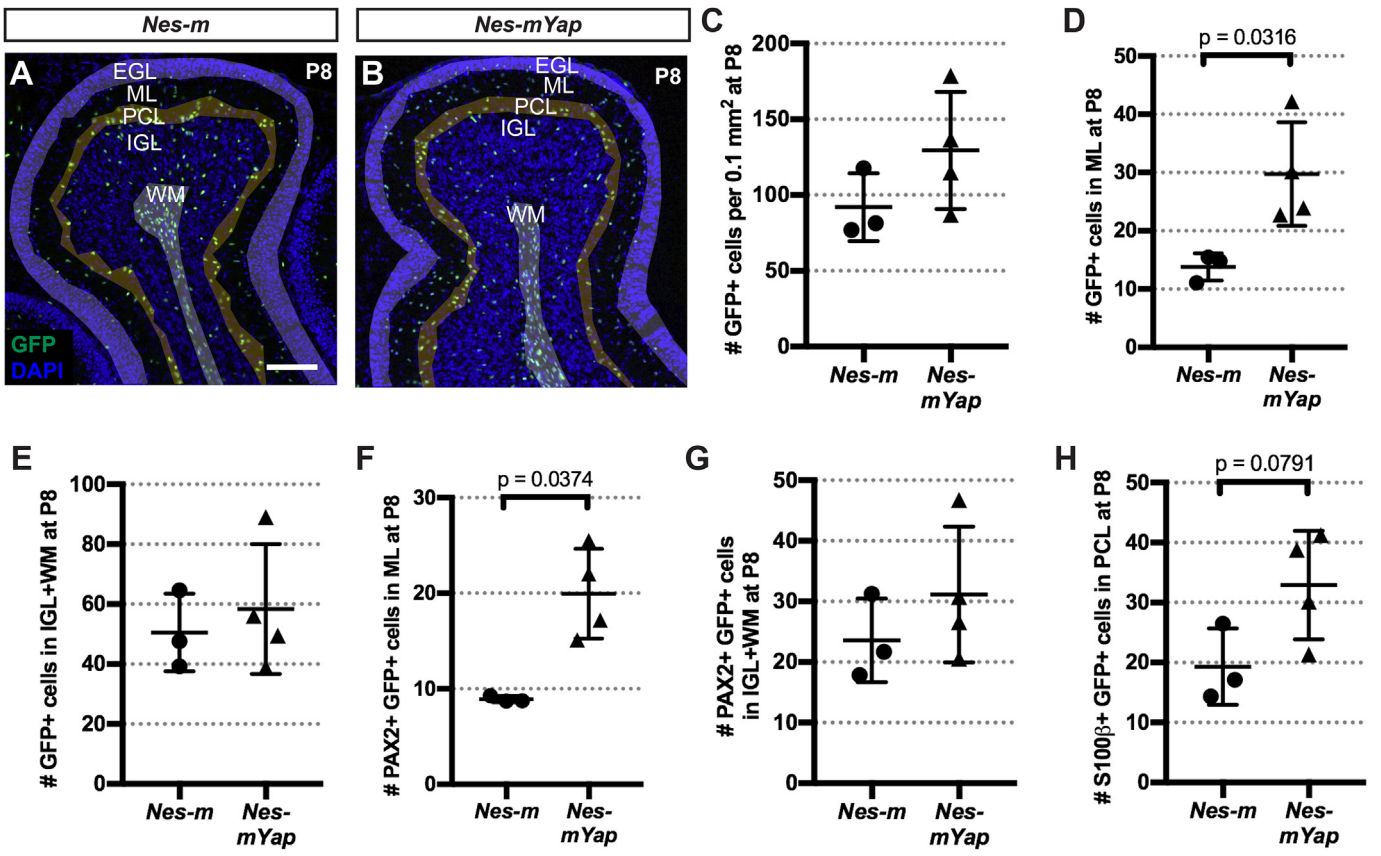

Fig. 4. YAP attenuates the differentiation of NEPs during normal postnatal cerebellar development. (A-B) Representative images from lobule 4/5 showing IF staining of GFP and DAPI on midsagittal sections from a *Nes-m* control and a *Nes-mYap* cKO at P8. Shading indicates the partitioning of the different layers (EGL, ML, PCL, IGL and WM) within the lobule. Scale bar, 100 μm. (C-H) Graphs of the numbers of GFP+ cells in all the layers (C) or in the ML (D) or IGL + WM (E), and the numbers of PAX2+ GFP+ cells in the ML (F) and IGL + WM (G), and the numbers of S100β+ GFP+ cells in the PCL (H), per 0.1 mm^2 of the total area analyzed in lobule 4/5 from *Nes-m* controls (n = 3) and *Nes-mYap* cKOs (n = 4) at P8. (C) P = 0.1996; (E) P = 0.6065; (G) P = 0.3548. Statistical analysis is conducted by unpaired *t*-test. Data are presented as mean ± standard deviation (S.D.), and each data point represents one animal.

during injury-induced recovery.

3.7. YAP is not required in GCPs for cerebellar growth during normal development

Given that when *Yap* is deleted in NEPs there is an increase in cell death of GCPs at P12 in IR cerebella, one possible explanation is that YAP is required for GCP proliferation/differentiation or survival. In order to determine whether YAP plays a role in GCPs during normal development of the cerebellum, we generated two mutants. First, we deleted *Yap* from the ATOH1-expressing rhombic lip lineage when GCPs are generated in the embryo and analyzed the size of the cerebellum at P30. Similar to mice lacking *Yap* in NEPs (Fig. 2C,D), P30 *Atoh1-Cre/+;Yap*$^{flox/flox}$ (*Atoh1-Yap* cKO) mice showed no reduction in the area of the midline cerebellum (Fig. 6A and B), or the IGL area or IGL/cerebellum ratio compared to *Yap*$^{flox/flox}$ littermate controls (Fig. 6C-G). This lack of a growth phenotype shows that YAP does not play a major role in the *Atoh1*-lineage for growth of the cerebellum during development.

We next used the MASTR mosaic mutant approach with an *Atoh1-FlpoER* transgene (Wojcinski et al., 2019) as a sensitive assay for a mild change in differentiation of GCPs when *Yap* is removed. Tm was administered at P0 to *Atoh1-FlpoER/+;R26*$^{FSF\text{-}GFPcre/+}$*;Yap*$^{flox/flox}$ (*Atoh1-mYap* cKO) mice and controls (*Atoh1-FlpoER/+;R26*$^{FSF\text{-}GFPcre/+}$ or *Atoh1-m*), and then EdU was injected 1 h prior to sacrifice at P8. The EdU+ outer EGL (oEGL) consists of actively proliferating GCPs. The percentage of post-mitotic GFP+ granule cells was quantified in the EdU-negative "inner layers" including the inner EGL (iEGL), ML, IGL, and WM as a percentage of all GFP+ cells (Fig. 6H-I, H′-I′). Interestingly, we found that the percentage of GFP+ postmitotic cells in the "inner layers" was slightly but significantly higher in *Atoh1-mYap* cKOs compared to *Atoh1-m* controls (Fig. 6J), indicating an increase in differentiation, or decrease in self-renewal of GCPs. The proliferation index (percent of EdU+ GFP+ cells among all GFP+ cells in the oEGL) was similar between GFP+ *Atoh1-mYap* cKO cells and *Atoh1-m* control GCPs (Fig. 6K), showing that *Yap* does not regulate the proliferation rate. Taken together, these data indicate that YAP plays only a minor role in attenuating differentiation of GCPs into granule neurons.

3.8. Loss of Taz in Yap mutant NEPs does not abrogate recovery after irradiation

Since TAZ and YAP have been found to have both similar and distinct requirements in the development or regeneration of various organs (Deng et al., 2016; Hossain et al., 2007; Makita et al., 2008; Morin-Kensicki et al., 2006; Reginensi et al., 2013; Tian et al., 2007), and we detected nuclear TAZ in NEPs (Fig. 1C-D,C′-D′, C″-D″), we asked whether TAZ contributes to the regenerative response following irradiation in *Nes-mYap* cKOs. We first tested whether *Taz* alone is required for development and replenishment of the cerebellum after irradiation by administering Tm at P0 to *Nes-FlpoER/+;R26*$^{FSF\text{-}GFPcre/+}$*;Taz*$^{flox/flox}$ mice (*Nes-mTaz* cKOs) and controls (*Nes-FlpoER/+;Taz*$^{flox/flox}$, or *R26*$^{FSF\text{-}GFPcre/+}$*;Taz*$^{flox/flox}$, or *Taz*$^{flox/flox}$). Similar to *Nes-mYap* cKOs, conditional deletion of *Taz* did not alter cerebellar size at P30 (Fig. 7; Fig. 7S). However, unlike *Nes-mYap* cKOs, *Nes-mTaz* cKOs recovered almost as well as control mice after irradiation (Fig. 7; Fig. 7S).

We next ablated both *Yap* and *Taz* from NEPs using *Nes-FlpoER/*

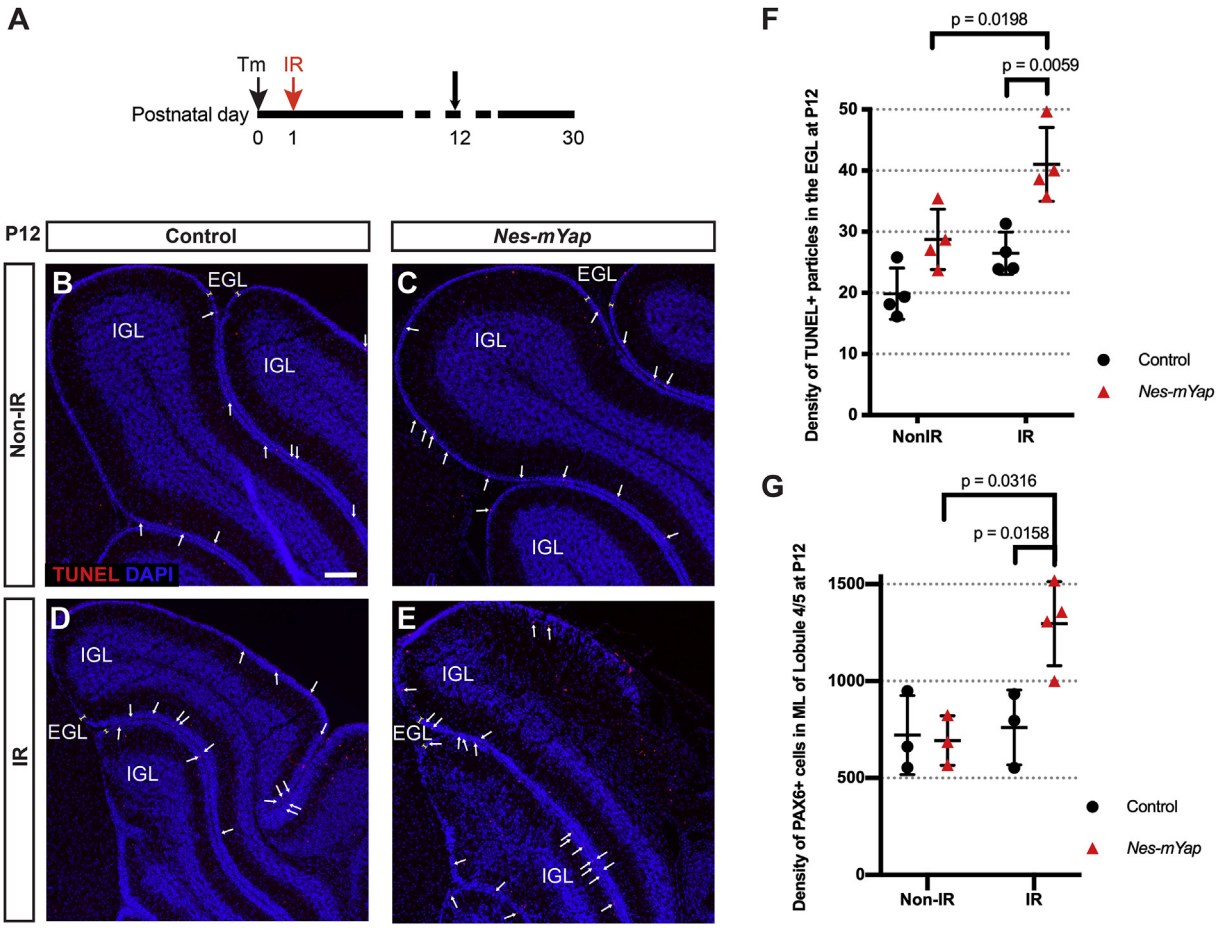

Fig. 5. Mutation of *Yap* in NEPs at P0 results in more cell death in the EGL and a defect in granule cell migration at P12 after irradiation-induced EGL injury at P1. (A) Schematic showing experimental design. (B-E) Representative images showing IF staining for TUNEL and DAPI on midsagittal sections from IR and Non-IR *Nes-mYap* cKOs and controls at P12. Arrows indicate TUNEL+ particles in the EGL. Scale bar, 100 μm. (F) Graph of the densities of TUNEL+ particles in the EGL (the number of TUNEL+ particles per 0.1 mm^2 of EGL area) in midline cerebellar sections from *Nes-mYap* cKOs (Non-IR, n = 3; IR, n = 4) and controls (Non-IR, n = 4; IR, n = 4) at P12. (G) Graph of the densities of PAX6+ cells in the ML (the number of PAX6+ cells per 1 mm^2 of ML area) in midline cerebellar sections from *Nes-mYap* cKOs (Non-IR, n = 3; IR, n = 3) and controls (Non-IR, n = 3; IR, n = 3) at P12. Data are presented as mean ± S.D., and statistical analysis by two-way ANOVA. Each data point represents one animal.

$+;R26^{FSF\text{-}GFPcre/+};Yap^{flox/flox};Taz^{flox/flox}$ mice (*Nes-mYapTaz* cKOs) and controls (*Nes-FlpoER/+*;$Yap^{flox/flox};Taz^{flox/flox}$ or $R26^{FSF\text{-}GFPcre/+};Yap^{flox/flox};Taz^{flox/flox}$ or $Yap^{flox/flox};Taz^{flox/flox}$) given Tm at P0. Surprisingly, ablation of both *Yap* and *Taz* did not result in a worse recovery of the cerebellum after injury compared to *Nes-mYap* cKOs. On the contrary, *Nes-mYapTaz* cKOs had no significant reduction in the area of the midline cerebellum or IGL, although they had a small but significant reduction in the IGL/cerebellum ratio compared to controls (Fig. 8; Figs. 8S1A–C). The genetic loss of *Yap* and *Taz* was confirmed via RT-qPCR analysis of the *Yap* and *Taz* mRNA levels in GFPcre+ NEPs isolated by FACS from *Nes-mYapTaz* cKO compared to *Nes-m* control mice at P8 (Fig. 8S2). Significantly, the mRNA expression of both genes was greatly reduced (Fig. 8S2). The apparent better recovery of *Nes-mYapTaz* cKOs compared to *Nes-mYap* cKOs could indicate that loss of *Taz* partially rescues the poor late recovery observed in *Nes-mYap* cKOs (Figs. 8S1D–F).

In order to examine whether the apparent better recovery in *Nes-mYapTaz* cKOs compared to *Nes-mYap* cKOs correlates with better survival of GCPs in the EGL at P12, we quantified cell death by TUNEL staining of cerebellar sections. Unlike the increase in the density of TUNEL+ particles within the EGL of P12 *Nes-mYap* cKOs compared to controls after irradiation (Fig. 5F), IR *Nes-mYapTaz* cKOs did not have a significant increase in cell death in the EGL compared to controls (Fig. 8S3). Such an attenuation of cell death could contribute to the slightly better regeneration observed in *Nes-mYapTaz* cKOs compared to *Nes-mYap* cKOs. Furthermore, the differentiation of NEPs was not altered in *Nes-mYapTaz* cKOs compared to controls at P8 in Non-IR mice (Fig. 8S4).

4. Discussion

We have demonstrated that YAP is required for postnatal regeneration of the cerebellum following irradiation at P1. In particular, mutation of *Yap* impairs the partial recovery of cerebellar size and formation of the IGL following irradiation, but not the adaptive reprogramming of NEPs (Fig. 9). The defect in regeneration of the IGL in *Nes-mYap* cKOs is accompanied by an increase in cell death in the EGL and accumulation of granule cells in the ML at P12, following normal initial expansion and migration of NEPs to the EGL in response to the injury (Fig. 9). The organizations of Purkinje cells and Bergmann glial fibers is disrupted in IR *Yap* mutants. It is possible that this aspect of the phenotype is a secondary result of the failure of the GCPs to generate an IGL in IR *Yap* mutants. Alternatively, *Yap* depletion in NEPs could result in a cell autonomous defect in Bergmann glia that is only critical following irradiation, and that cell non-autonomously reduces survival of GCPs and/or hinders the migration of granule cells into the IGL resulting in a depletion of the EGL. Consistent with the latter, granule cells only accumulate in lobules where recovery of the IGL is very poor and Bergmann glia are the most abnormal in mutants after irradiation (lobules 4/5 and not 9).

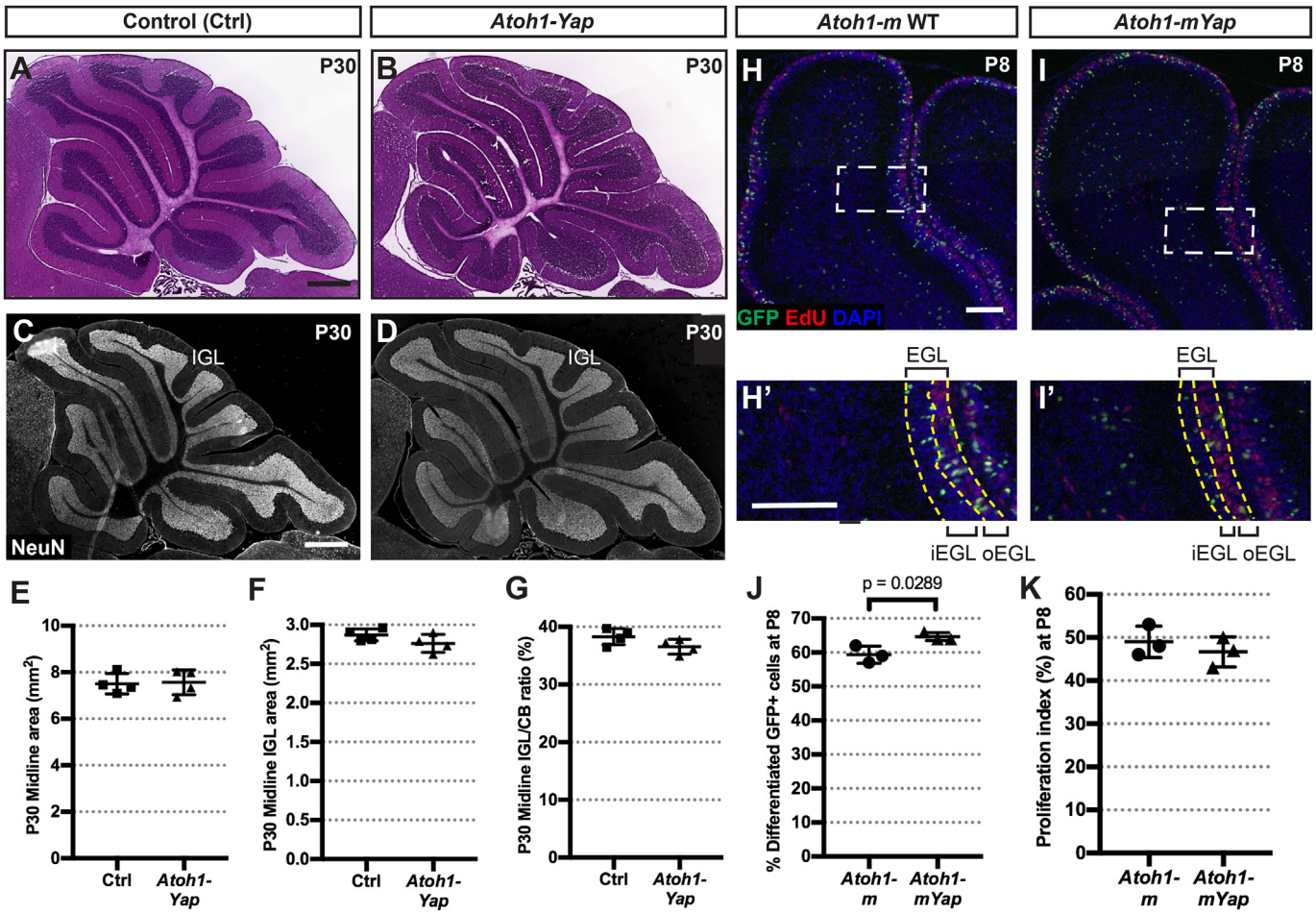

Fig. 6. YAP attenuates differentiation of GCPs during postnatal development of the cerebellum. (A-D) H&E staining (A-B) and IF detection of the granule cell marker NeuN (C-D) on midsagittal sections of cerebella from *Atoh1-Yap* cKOs and control (Ctrl) mice at P30. Scale bars, 500 μm. (E-G) Graphs of the areas of the midline of the cerebellum (E), the areas of the IGL (F), and IGL/cerebellum area ratios (G) of *Atoh1-Yap* cKO (n = 4) and littermate controls (n = 4) at P30. (E) p = 0.8554; (F) p = 0.1727; (G) p = 0.1155. (H-I) Representative images from lobule 4/5 showing IF staining for GFP, EdU, and DAPI on midsagittal sections from an *Atoh1-m* control and *Atoh1-mYap* cKO at P8 after TM at P0. (H′-I′) Magnification of areas within dotted lines in H-I. Yellow dashed lines indicate the EGL and the border of the outer- and inner-EGL. Scale bars, 100 μm. (J-K) Graphs of the percentages of GFP+ differentiating cells (in all layers except the proliferating oEGL) among all GFP+ cells (J) and proliferation indices (G) in the midline of the cerebella in *Atoh1-m* controls (n = 3) and *Atoh1-mYap* cKOs (n = 3) at P8. (K) P = 0.4670. Data are presented as mean ± S.D., and statistical analysis by unpaired *t*-test. Each data point represents one animal.

The pivotal role of Hippo signaling in brain development has been extensively studied in *Drosophila*, a model organism in which the Hippo pathway itself was first discovered. Drosophila lacking the YAP homolog Yorkie display semi-lethality and impaired proliferation and growth of neural stem cells at the larval stage (Ding et al., 2016). In a complementary manner, inhibition of Hippo signaling, through either over-expression of Yorkie or loss-of-function mutations in several core kinases that activate Yorkie function, results in increased neuroblast proliferation and substantial brain overgrowth (Poon et al., 2016). In the mouse, genetic ablation of *Yap* in radial glial progenitors leads to only subtle proliferation defects during cortical development (Park et al., 2016), whereas loss of both *Yap* and *Taz* results in a loss of ependymal cells that line the ventricle in the postnatal brain (W. A. Liu et al., 2018). Consistent with the subtle requirement for YAP in cortical development (Park et al., 2016), we found that *Yap* ablation from NEPs or GCPs does not significantly reduce the overall size of the adult cerebellum. We nevertheless observed mild increases in differentiation of *Yap* mutant NEPs and GCPs. In particular, removal of *Yap* from NEPs or GCPs in a mosaic manner in the cerebellum between P1 and P8 results in an increase in differentiation of NEPs (PCL-NEPs to produce Bergmann glia and WM-NEPs to produce interneurons) and GCPs (to produce granule cells) possibly at the expense of self-renewal. YAP seems to have a similar function in progenitor proliferation/differentiation in other organs. For example, YAP over-activation in mouse intestine or chick neural tube leads to expansion of progenitor cells and loss of differentiated cells (Camargo et al., 2007; Cao et al., 2008). It also has been shown that over-expression of YAP in cultured myoblasts inhibits differentiation and formation of myotubes (Watt et al., 2010), and reduced Hippo signaling in mouse epithelial cells results in hyper-proliferation of progenitors and failure of differentiation into multiple epithelial cell types (J. H. Lee et al., 2008). Thus, a consistent finding from our current study in the cerebellum and work of others in distinct organs is that YAP modulates a timely transition of progenitors from cell proliferation into differentiation.

Several lines of evidence suggest an intersection or coupling of the Hedgehog (HH) and Hippo pathways in *Drosophila* and mice (Akladios et al., 2017; Fernandez et al., 2009; Hsu et al., 2017; Huang and Kalderon, 2014; Lin et al., 2012). For example, in flies elevated Hh signaling (*ptc* mutants) induces Yorkie target gene transcription, whereas additional deletion of Yorkie abolishes the effects of excess Hh signaling on cell proliferation and survival (Huang and Kalderon, 2014). In cultured mouse GCPs, SHH treatment was reported to increase the transcription and nuclear localization of YAP protein (Fernandez et al., 2009). Our previous study showed that SHH signaling is required for NEPs to

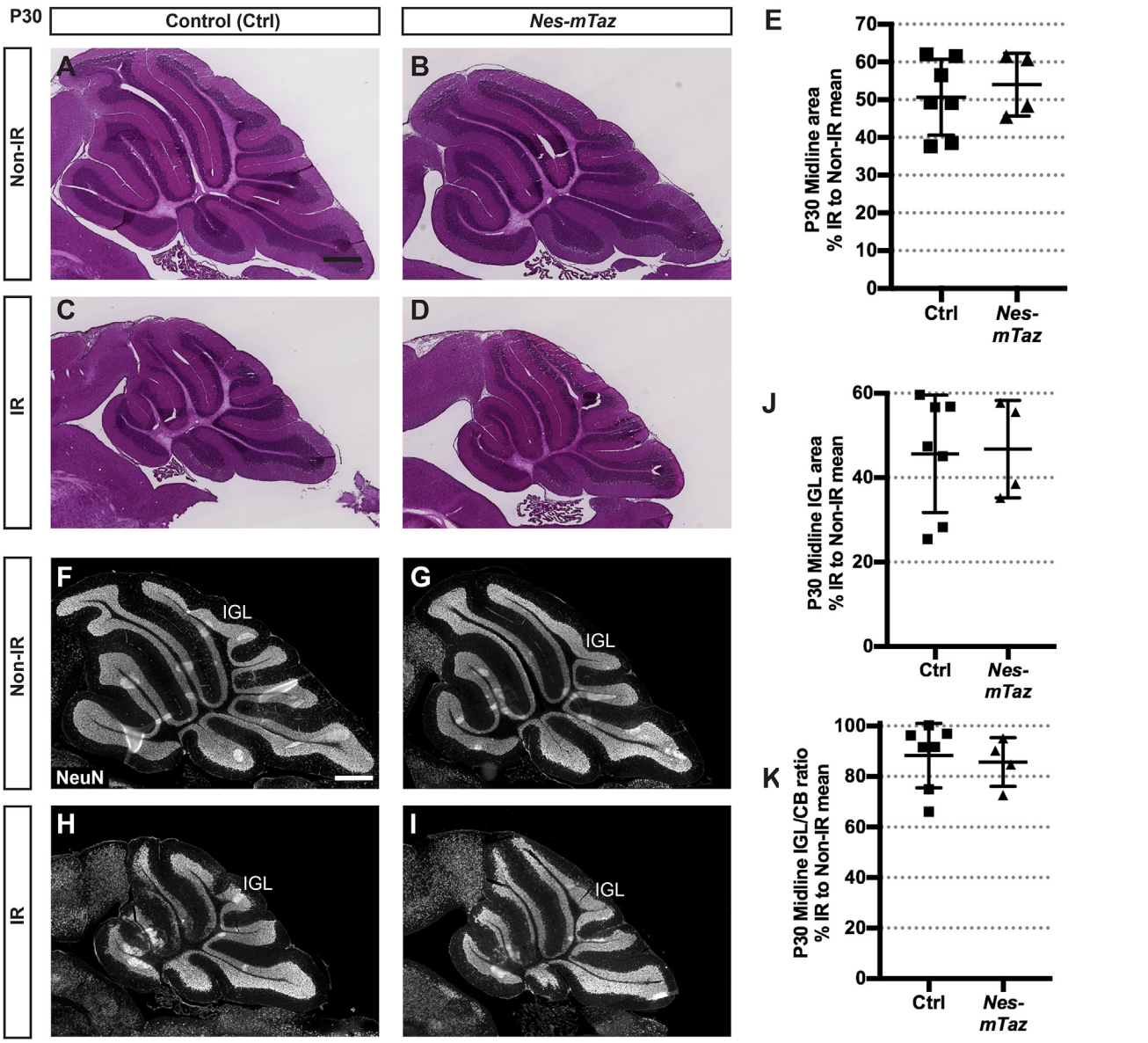

Fig. 7. Mutation of *Taz* in NEPs at P0 does not alter cerebellar growth during development and regeneration after irradiation at P1. (A-D) H&E staining of midsagittal sections of cerebella from Non-IR and IR of *Nes-mTaz* cKOs and controls at P30. Scale bars, 500 μm. (E) Graph of the areas of the cerebella of IR animals as a percentage of Non-IR mice of the same genotype in midline sections. $p = 0.5866$. (F-I) IF detection of NeuN on midsagittal sections of the cerebella from Non-IR and IR *Nes-mTaz* cKOs and controls at P30. Scale bar, 500 μm. (J,K) Graphs of the IGL areas (J) and IGL/cerebellum ratios (K) of IR *Nes-mTaz* cKOs (Non-IR, $n = 6$; IR, $n = 4$) and controls (Non-IR, $n = 4$; IR, $n = 7$) at P30 as a percentage of Non-IR same genotype. (J) $p = 0.8945$; (K) $p = 0.7335$. Data are presented as mean ± S.D., and statistical analysis by unpaired *t*-test. Each data point represents one animal and is calculated using each IR measurement divided by the mean of Non-IR mice of the same genotype, X 100.

regenerate the IR mouse cerebellum, particularly at the initial stage of recovery (Wojcinski et al., 2017). Thus, it is possible that SHH signaling after irradiation activates YAP function and this promotes survival of NEPs immediately after irradiation, since we observed an increase in cell death after irradiation in the PCL of mutants where NEPs are the main proliferating cell type. However, comparison of *Nes-mSmo* cKO (Wojcinski et al., 2017) and *Nes-mYap* cKO phenotypes after irradiation of the cerebellum reveals additional requirements for SHH signaling that are independent of *Yap*. In *Nes-mSmo* cKOs there is an immediate defect in expansion of NEPs and their migration to the EGL after irradiation (Wojcinski et al., 2017), whereas these cellular responses are intact in *Nes-mYap* cKOs. Taken together, the results provide evidence that SHH has critical target genes other than *Yap* that are required for proliferation and migration of NEPs.

YAP and TAZ have often been found to have overlapping functions, consistent with their significant homology and common binding partners, but some recent studies point to distinct roles in addition to overlapping functions of YAP and TAZ that appear to be context dependent. For example, *Yap* null mutant mice are embryonical lethals (Morin-Kensicki et al., 2006), whereas *Taz* nulls only show partial embryonic lethality and mice that survive have lung defects and kidney disease (Hossain et al., 2007; Makita et al., 2008; Tian et al., 2007). It has also been shown that TAZ competes with YAP in an interaction with a regulator protein that modulates the maturation of chondrocytes, a critical step for skeletal development and bone repair (Deng et al., 2016). Similarly, we found that *Yap* ablation from NEPs leads to poor recovery of the postnatal cerebellum following acute injury, but deletion of *Taz* does not abrogate regeneration. Furthermore, double conditional *Yap* and *Taz*

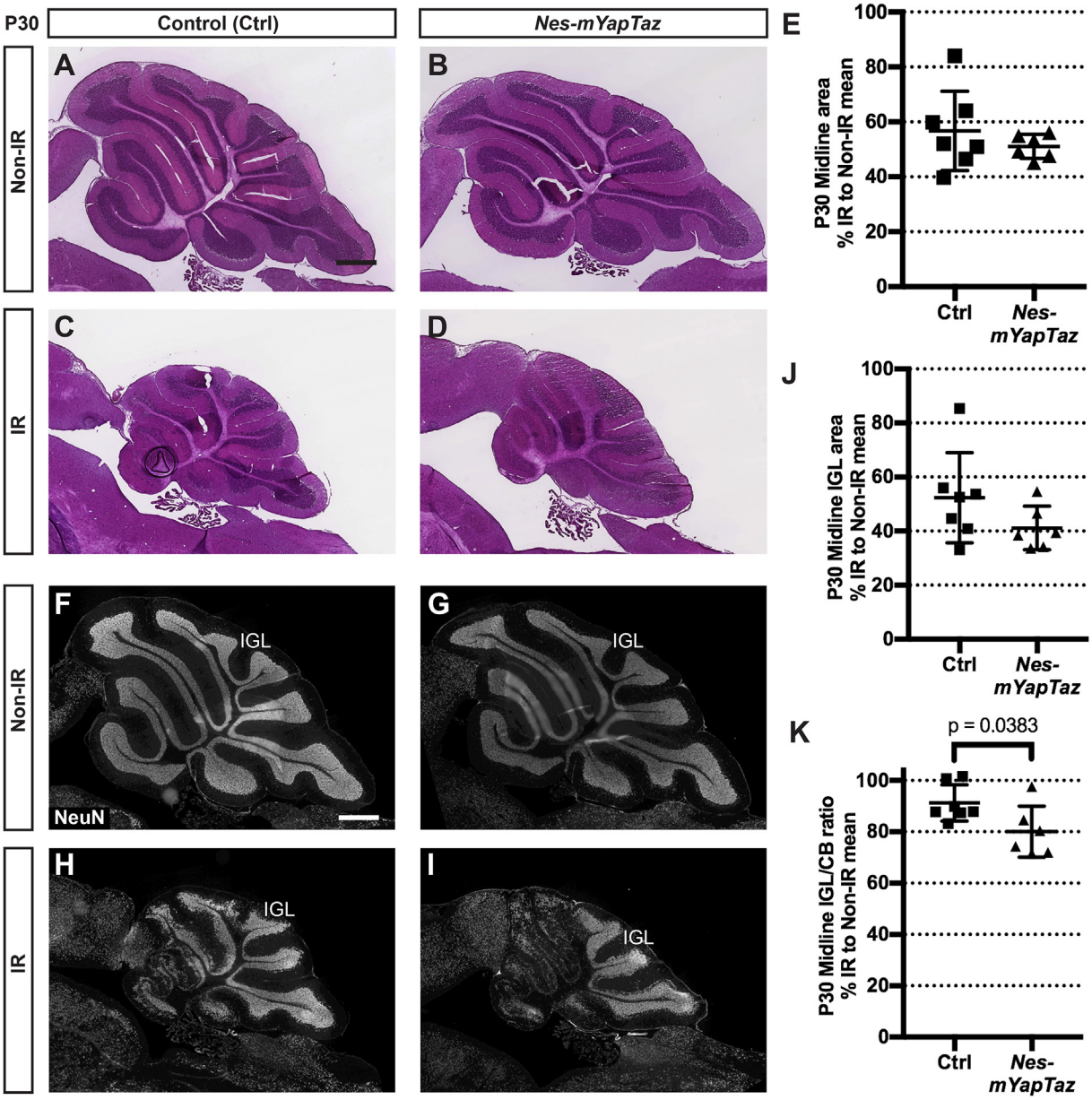

Fig. 8. Loss of *Taz* in NEPs lacking *Yap* at P0 does not abrogate recovery of the IGL after irradiation at P1. (A-D) H&E staining of midsagittal sections of the cerebella from Non-IR and IR *Nes-mYapTaz* cKOs and controls at P30. Scale bars, 500 μm. (E) Graph of the midline cerebellar areas of IR mice as a percentage of Non-IR animals of the same genotype. P = 0.3815. (F-I) IF detection of NeuN on midsagittal sections of the cerebella from Non-IR and IR animals at P30. Scale bar, 500 μm. (J,K) Graphs of the areas of the IGL (J) and IGL/cerebellum ratios (K) of IR mice as a percentage of Non-IR animals of the same genotype on midsaggital sections at P30. *Nes-mYapTaz* cKOs (Non-IR, n = 7; IR, n = 6) and controls (Non-IR, n = 4; IR, n = 7). (J) p = 0.1637; (K) p = 0.0383. Data are presented as mean ± S.D., and statistical analysis by unpaired *t*-test. Each data point represents one animal and is calculated using the average for each IR mouse divided by the mean of the Non-IR mice of the same genotype, X 100.

mutants appear to have a milder phenotype than *Yap* cKOs, indicating that loss of *Taz* partially rescues the *Yap* mutant phenotype. This finding raises the possibility of antagonistic functions between YAP and TAZ in NEPs, as in the bone, compared to overlapping functions under other circumstances. It is also possible that differences in the genetic backgrounds of the single and double mutants contribute to the degree of recovery of *Yap* mutant NEPs after irradiation. Thus, it will be important to dissect the distinct downstream molecular pathways of the two co-activators to reveal their context-dependent functions in the Hippo pathway. Leveraging this knowledge will pave the road for potential therapeutic intervention for cerebellar hypoplasia caused by injury.

5. Conclusions

YAP but not TAZ is required for postnatal regeneration of the cerebellum following irradiation at P1 at the level of promoting production of the granule cells that make up the IGL. YAP is not required for the initial adaptive reprogramming of NEPs or migration of NEP-derived cells to the EGL following irradiation. YAP plays a role in cell survival following irradiation, first in the PCL at P2 and then in the EGL at P12. YAP also seems to promote migration of granule cells from the EGL to the IGL at P12 in IR mice. YAP normally plays only a minor role during development in attenuating differentiation of NEPs and GCPs. Finally, TAZ does not appear to have an overlapping function with YAP in NEPs.

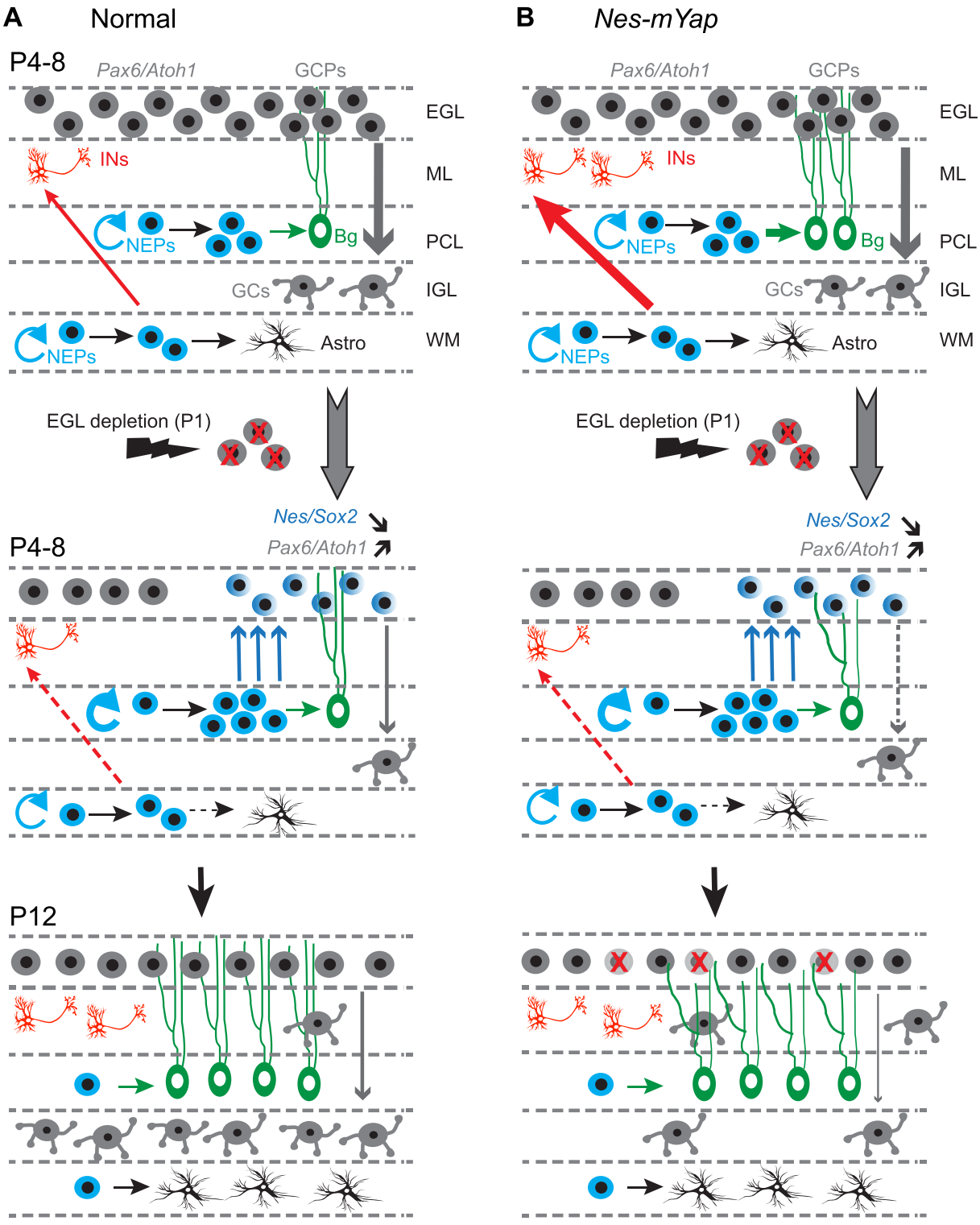

Fig. 9. Model of the cellular responses during the development and regeneration of neonatal cerebellum in normal and *Nes-mYap* mice after irradiation at P1. (A) Depletion of the External Granule Layer (EGL) during the first days of postnatal cerebellar development results in an expansion and migration of *Nestin*-Expressing Progenitors (NEPs) in the Purkinje Cell Layer (PCL) that normally produce Astrocytes (Astro) and Bergmann Glia (Bg). Once in the EGL, NEP-derived cells initiate expression of Granule Cell lineage-specific genes (*Pax6* and *Atoh1*) and expand to replenish the EGL. Concomitantly, white matter (WM) NEPs have a transient reduction in production of interneurons (INs) and astrocytes. (B) In Non-IR *Nes-mYap* mice, the growth of cerebella is not altered during development, with normal cerebellar size and internal granule cell layer (IGL). Genetic ablation of *Yap* from NEPs promotes the differentiation of WM-NEPs into interneurons in the molecular layer (ML), and the differentiation of PCL-NEPs into astrocytes. In IR *Nes-mYap* mice, depletion of the EGL at P1 leads to the expansion of NEPs in the PCL and migration to the EGL. GCPs in *Nes-mYap* mice have increased cell death and defective migration into the IGL compared to that in control mice, possibly because the Bergmann glia are defective. These defects in the granule cell lineage contribute to the poor recovery of the IGL that has much fewer granule cells (GCs). The slight enhancement of differentiation of *Yap* mutant NEPs, however, is overridden in IR cerebella.

Conflicts of interest

The authors declare no competing or financial interests.

Author contributions

A.L.J. helped design the study, interpret the data, write the manuscript and supervised the project. Z.Y. helped design the study, and analyze and interpret the data. Z.Y. also performed most of the experiments and wrote a first draft of the manuscript.

Funding

This work was supported by a grant from the National Institutes of Health to A.L.J. [NS092096], and a National Cancer Institute Cancer Center Support Grant [P30 CA008748-48].

Acknowledgements

We thank Dr. Jeff Wrana for providing the *Yap* and *Taz* conditional mutant mice via Dr. Kathryn Anderson's lab. We thank Dr. Alexandre Wojcinski for insightful suggestions on experimental design and interpretation of results, and Dr. I-Li Tan for performing one RT-qPCR experiment. We are grateful to Daniel Stephen and Zhimin Lao for technical assistance. We thank all the Joyner lab members for their helpful comments and discussions. We also thank the Flow Cytometry core and the Center for Comparative Medicine and Pathology of MSKCC for outstanding technical support. We gratefully acknowledge P. Zanzonico for his help with mouse irradiation; Q. Chen and the MSKCC Small-Animal Imaging Core Facility for technical assistance; and a Shared Resources Grant from the MSKCC Geoffrey Beene Cancer Research Center, which provided funding support for the purchase of the XRad 225Cx Microirradiator.

Appendix A. Supplementary data

Supplementary data to this article can be found online at https://doi.org/10.1016/j.ydbio.2019.07.018.

References

Akladios, B., Mendoza Reinoso, V., Cain, J.E., Wang, T., Lambie, D.L., Watkins, D.N., Beverdam, A., 2017. Positive regulatory interactions between YAP and Hedgehog signalling in skin homeostasis and BCC development in mouse skin in vivo. PLoS One 12 (8), e0183178. https://doi.org/10.1371/journal.pone.0183178.

Altman, J., Anderson, W.J., Wright, K.A., 1969. Early effects of x-irradiation of the cerebellum in infant rats: decimation and reconstitution of the external granular layer. Exp. Neurol. 24 (2), 196–216.

Altman, J., Bayer, S.A., 1997. Development of the Cerebellar System in Relation to its Evolution, Structure, and Functions. CRC Press, Boca Raton.

Andreotti, J.P., Prazeres, P., Magno, L.A.V., Romano-Silva, M.A., Mintz, A., Birbrair, A., 2018. Neurogenesis in the postnatal cerebellum after injury. Int. J. Dev. Neurosci. 67, 33–36. https://doi.org/10.1016/j.ijdevneu.2018.03.002.

Ardestani, A., Maedler, K., 2018. The hippo signaling pathway in pancreatic beta-cells: functions and regulations. Endocr. Rev. 39 (1), 21–35. https://doi.org/10.1210/er.2017-00167.

Bayin, N.S., Wojcinski, A., Mourton, A., Saito, H., Suzuki, N., Joyner, A.L., 2018. Age-dependent dormant resident progenitors are stimulated by injury to regenerate Purkinje neurons. Elife 7. https://doi.org/10.7554/eLife.39879.

Biran, V., Verney, C., Ferriero, D.M., 2012. Perinatal cerebellar injury in human and animal models. Neurol Res Int 858929. https://doi.org/10.1155/2012/858929. *2012*.

Brossard-Racine, M., du Plessis, A.J., Limperopoulos, C., 2015. Developmental cerebellar cognitive affective syndrome in ex-preterm survivors following cerebellar injury. Cerebellum 14 (2), 151–164. https://doi.org/10.1007/s12311-014-0597-9.

Buffo, A., Rossi, F., 2013. Origin, lineage and function of cerebellar glia. Prog. Neurobiol. 109, 42–63. https://doi.org/10.1016/j.pneurobio.2013.08.001.

Callus, B.A., Verhagen, A.M., Vaux, D.L., 2006. Association of mammalian sterile twenty kinases, Mst1 and Mst2, with hSalvador via C-terminal coiled-coil domains, leads to its stabilization and phosphorylation. FEBS J. 273 (18), 4264–4276. https://doi.org/10.1111/j.1742-4658.2006.05427.x.

Camargo, F.D., Gokhale, S., Johnnidis, J.B., Fu, D., Bell, G.W., Jaenisch, R., Brummelkamp, T.R., 2007. YAP1 increases organ size and expands undifferentiated progenitor cells. Curr. Biol. 17 (23), 2054–2060. https://doi.org/10.1016/j.cub.2007.10.039.

Cao, X., Pfaff, S.L., Gage, F.H., 2008. YAP regulates neural progenitor cell number via the TEA domain transcription factor. Genes Dev. 22 (23), 3320–3334. https://doi.org/10.1101/gad.1726608.

Cerrato, V., Parmigiani, E., Figueres-Onate, M., Betizeau, M., Aprato, J., Nanavaty, I., Buffo, A., 2018. Multiple origins and modularity in the spatiotemporal emergence of cerebellar astrocyte heterogeneity. PLoS Biol. 16 (9), e2005513 https://doi.org/10.1371/journal.pbio.2005513.

Chan, E.H., Nousiainen, M., Chalamalasetty, R.B., Schafer, A., Nigg, E.A., Sillje, H.H., 2005. The Ste20-like kinase Mst2 activates the human large tumor suppressor kinase Lats1. Oncogene 24 (12), 2076–2086. https://doi.org/10.1038/sj.onc.1208445.

Chen, P., Johnson, J.E., Zoghbi, H.Y., Segil, N., 2002. The role of Math1 in inner ear development: uncoupling the establishment of the sensory primordium from hair cell fate determination. Development 129 (10), 2495–2505.

Corrales, J.D., Blaess, S., Mahoney, E.M., Joyner, A.L., 2006. The level of sonic hedgehog signaling regulates the complexity of cerebellar foliation. Development 133 (9), 1811–1821. https://doi.org/10.1242/dev.02351.

Corrales, J.D., Rocco, G.L., Blaess, S., Guo, Q., Joyner, A.L., 2004. Spatial pattern of sonic hedgehog signaling through Gli genes during cerebellum development. Development 131 (22), 5581–5590. https://doi.org/10.1242/dev.01438.

Deng, Y., Wu, A., Li, P., Li, G., Qin, L., Song, H., Mak, K.K., 2016. Yap1 regulates multiple steps of chondrocyte differentiation during skeletal development and bone repair. Cell Rep. 14 (9), 2224–2237. https://doi.org/10.1016/j.celrep.2016.02.021.

Ding, R., Weynans, K., Bossing, T., Barros, C.S., Berger, C., 2016. The Hippo signalling pathway maintains quiescence in Drosophila neural stem cells. Nat. Commun. 7, 10510. https://doi.org/10.1038/ncomms10510.

Dobbing, J., Sands, J., 1973. Quantitative growth and development of human brain. Arch. Dis. Child. 48 (10), 757–767.

Emoto, K., 2011. The growing role of the Hippo–NDR kinase signalling in neuronal development and disease. J. Biochem. 150 (2), 133–141. https://doi.org/10.1093/jb/mvr080.

Fatemi, S.H., Aldinger, K.A., Ashwood, P., Bauman, M.L., Blaha, C.D., Blatt, G.J., et al., 2012. Consensus paper: pathological role of the cerebellum in autism. Cerebellum 11 (3), 777–807. https://doi.org/10.1007/s12311-012-0355-9.

Fernandez, L.A., Northcott, P.A., Dalton, J., Fraga, C., Ellison, D., Angers, S., Kenney, A.M., 2009. YAP1 is amplified and up-regulated in hedgehog-associated medulloblastomas and mediates Sonic hedgehog-driven neural precursor proliferation. Genes Dev. 23 (23), 2729–2741. https://doi.org/10.1101/gad.1824509.

Fernandez, L.A., Squatrito, M., Northcott, P., Awan, A., Holland, E.C., Taylor, M.D., et al., 2012. Oncogenic YAP promotes radioresistance and genomic instability in medulloblastoma through IGF2-mediated Akt activation. Oncogene 31 (15), 1923–1937. https://doi.org/10.1038/onc.2011.379.

Fleming, J.T., He, W., Hao, C., Ketova, T., Pan, F.C., Wright, C.C., et al., 2013. The Purkinje neuron acts as a central regulator of spatially and functionally distinct cerebellar precursors. Dev. Cell 27 (3), 278–292. https://doi.org/10.1016/j.devcel.2013.10.008.

Halder, G., Johnson, R.L., 2011. Hippo signaling: growth control and beyond. Development 138 (1), 9–22. https://doi.org/10.1242/dev.045500.

Hortensius, L.M., Dijkshoorn, A.B.C., Ecury-Goossen, G.M., Steggerda, S.J., Hoebeek, F.E., Benders, M., Dudink, J., 2018. Neurodevelopmental consequences of preterm isolated cerebellar hemorrhage: a systematic review. Pediatrics 142 (5). https://doi.org/10.1542/peds.2018-0609.

Hossain, Z., Ali, S.M., Ko, H.L., Xu, J., Ng, C.P., Guo, K., et al., 2007. Glomerulocystic kidney disease in mice with a targeted inactivation of Wwtr1. Proc. Natl. Acad. Sci. U. S. A. 104 (5), 1631–1636. https://doi.org/10.1073/pnas.0605266104.

Hsu, T.H., Yang, C.Y., Yeh, T.H., Huang, Y.C., Wang, T.W., Yu, J.Y., 2017. The Hippo pathway acts downstream of the Hedgehog signaling to regulate follicle stem cell maintenance in the Drosophila ovary. Sci. Rep. 7 (1), 4480. https://doi.org/10.1038/s41598-017-04052-6.

Hu, J.K., Du, W., Shelton, S.J., Oldham, M.C., DiPersio, C.M., Klein, O.D., 2017. An FAK-YAP-mTOR signaling Axis regulates stem cell-based tissue renewal in mice. Cell Stem Cell 21 (1), 91–106. https://doi.org/10.1016/j.stem.2017.03.023 e106.

Huang, J., Kalderon, D., 2014. Coupling of Hedgehog and Hippo pathways promotes stem cell maintenance by stimulating proliferation. J. Cell Biol. 205 (3), 325–338. https://doi.org/10.1083/jcb.201309141.

Ikeda, S., Sadoshima, J., 2016. Regulation of myocardial cell growth and death by the hippo pathway. Circ. J. 80 (7), 1511–1519. https://doi.org/10.1253/circj.CJ-16-0476.

Jaeger, B.N., Jessberger, S., 2017. Unexpected help to repair the cerebellum. Nat. Neurosci. 20 (10), 1319–1321. https://doi.org/10.1038/nn.4640.

Lao, Z., Raju, G.P., Bai, C.B., Joyner, A.L., 2012. MASTR: a technique for mosaic mutant analysis with spatial and temporal control of recombination using conditional floxed alleles in mice. Cell Rep. 2 (2), 386–396. https://doi.org/10.1016/j.celrep.2012.07.004.

Lavado, A., Park, J.Y., Pare, J., Finkelstein, D., Pan, H., Xu, B., et al., 2018. The hippo pathway prevents YAP/TAZ-Driven hypertranscription and controls neural progenitor number. Dev. Cell 47 (5), 576–591.e578. https://doi.org/10.1016/j.devcel.2018.09.021.

Lee, J.H., Kim, T.S., Yang, T.H., Koo, B.K., Oh, S.P., Lee, K.P., et al., 2008. A crucial role of WW45 in developing epithelial tissues in the mouse. EMBO J. 27 (8), 1231–1242. https://doi.org/10.1038/emboj.2008.63.

Lee, M., Goraya, N., Kim, S., Cho, S.H., 2018. Hippo-yap signaling in ocular development and disease. Dev. Dynam. 247 (6), 794–806. https://doi.org/10.1002/dvdy.24628.

Lewis, P.M., Gritli-Linde, A., Smeyne, R., Kottmann, A., McMahon, A.P., 2004. Sonic hedgehog signaling is required for expansion of granule neuron precursors and patterning of the mouse cerebellum. Dev. Biol. 270 (2), 393–410. https://doi.org/10.1016/j.ydbio.2004.03.007.

Li, P., Du, F., Yuelling, L.W., Lin, T., Muradimova, R.E., Tricarico, R., et al., 2013. A population of Nestin-expressing progenitors in the cerebellum exhibits increased tumorigenicity. Nat. Neurosci. 16 (12), 1737–1744. https://doi.org/10.1038/nn.3553.

Limperopoulos, C., Bassan, H., Gauvreau, K., Robertson Jr., R.L., Sullivan, N.R., Benson, C.B., duPlessis, A.J., 2007. Does cerebellar injury in premature infants contribute to the high prevalence of long-term cognitive, learning, and behavioral disability in survivors? Pediatrics 120 (3), 584–593. https://doi.org/10.1542/peds.2007-1041.

Lin, Y.T., Ding, J.Y., Li, M.Y., Yeh, T.S., Wang, T.W., Yu, J.Y., 2012. YAP regulates neuronal differentiation through Sonic hedgehog signaling pathway. Exp. Cell Res. 318 (15), 1877–1888. https://doi.org/10.1016/j.yexcr.2012.05.005.

Liu, W.A., Chen, S., Li, Z., Lee, C.H., Mirzaa, G., Dobyns, W.B., et al., 2018. PARD3 dysfunction in conjunction with dynamic HIPPO signaling drives cortical enlargement with massive heterotopia. Genes Dev. 32 (11-12), 763–780. https://doi.org/10.1101/gad.313171.118.

Liu, Y., Deng, J., 2019. Ubiquitinationdeubiquitination in the hippo signaling pathway (review). Oncol. Rep. 41 (3), 1455–1475. https://doi.org/10.3892/or.2019.6956.

Lu, L., Finegold, M.J., Johnson, R.L., 2018. Hippo pathway coactivators Yap and Taz are required to coordinate mammalian liver regeneration. Exp. Mol. Med. 50 (1), e423. https://doi.org/10.1038/emm.2017.205.

Makita, R., Uchijima, Y., Nishiyama, K., Amano, T., Chen, Q., Takeuchi, T., et al., 2008. Multiple renal cysts, urinary concentration defects, and pulmonary emphysematous changes in mice lacking TAZ. Am. J. Physiol. Renal. Physiol. 294 (3), F542–F553. https://doi.org/10.1152/ajprenal.00201.2007.

Marek, S., Siegel, J.S., Gordon, E.M., Raut, R.V., Gratton, C., Newbold, D.J., et al., 2018. Spatial and temporal organization of the individual human cerebellum. Neuron 100 (4), 977–993.e7. https://doi.org/10.1016/j.neuron.2018.10.010.

Matei, V., Pauley, S., Kaing, S., Rowitch, D., Beisel, K.W., Morris, K., et al., 2005. Smaller inner ear sensory epithelia in Neurog 1 null mice are related to earlier hair cell cycle exit. Dev. Dynam. 234 (3), 633–650. https://doi.org/10.1002/dvdy.20551.

Messerschmidt, A., Fuiko, R., Prayer, D., Brugger, P.C., Boltshauser, E., Zoder, G., et al., 2008. Disrupted cerebellar development in preterm infants is associated with impaired neurodevelopmental outcome. Eur. J. Pediatr. 167 (10), 1141–1147. https://doi.org/10.1007/s00431-007-0647-0.

Mignone, J.L., Kukekov, V., Chiang, A.S., Steindler, D., Enikolopov, G., 2004. Neural stem and progenitor cells in nestin-GFP transgenic mice. J. Comp. Neurol. 469 (3), 311–324. https://doi.org/10.1002/cne.10964.

Milosevic, A., Goldman, J.E., 2004. Potential of progenitors from postnatal cerebellar neuroepithelium and white matter: lineage specified vs. multipotent fate. Mol. Cell. Neurosci. 26 (2), 342–353. https://doi.org/10.1016/j.mcn.2004.02.008.

Morin-Kensicki, E.M., Boone, B.N., Howell, M., Stonebraker, J.R., Teed, J., Alb, J.G., Milgram, S.L., 2006. Defects in yolk sac vasculogenesis, chorioallantoic fusion, and embryonic axis elongation in mice with targeted disruption of Yap65. Mol. Cell. Biol. 26 (1), 77–87. https://doi.org/10.1128/mcb.26.1.77-87.2006.

Nguyen, T.H., Kugler, J.M., 2018. Ubiquitin-dependent regulation of the mammalian hippo pathway: therapeutic implications for cancer. Cancers 10 (4). https://doi.org/10.3390/cancers10040121.

Pan, D., 2010. The hippo signaling pathway in development and cancer. Dev. Cell 19 (4), 491–505. https://doi.org/10.1016/j.devcel.2010.09.011.

Park, R., Moon, U.Y., Park, J.Y., Hughes, L.J., Johnson, R.L., Cho, S.H., Kim, S., 2016. Yap is required for ependymal integrity and is suppressed in LPA-induced hydrocephalus. Nat. Commun. 7, 10329. https://doi.org/10.1038/ncomms10329.

Parmigiani, E., Leto, K., Rolando, C., Figueres-Onate, M., Lopez-Mascaraque, L., Buffo, A., Rossi, F., 2015. Heterogeneity and bipotency of astroglial-like cerebellar progenitors along the interneuron and glial lineages. J. Neurosci. 35 (19), 7388–7402. https://doi.org/10.1523/jneurosci.5255-14.2015.

Poon, C.L., Mitchell, K.A., Kondo, S., Cheng, L.Y., Harvey, K.F., 2016. The hippo pathway regulates neuroblasts and brain size in Drosophila melanogaster. Curr. Biol. 26 (8), 1034–1042. https://doi.org/10.1016/j.cub.2016.02.009.

Rakic, P., Sidman, R.L., 1970. Histogenesis of cortical layers in human cerebellum, particularly the lamina dissecans. J. Comp. Neurol. 139 (4), 473–500. https://doi.org/10.1002/cne.901390407.

Reginensi, A., Scott, R.P., Gregorieff, A., Bagherie-Lachidan, M., Chung, C., Lim, D.S., McNeill, H., 2013. Yap- and Cdc42-dependent nephrogenesis and morphogenesis during mouse kidney development. PLoS Genet. 9 (3), e1003380 https://doi.org/10.1371/journal.pgen.1003380.

Sillitoe, R.V., Joyner, A.L., 2007. Morphology, molecular codes, and circuitry produce the three-dimensional complexity of the cerebellum. Annu. Rev. Cell Dev. Biol. 23, 549–577. https://doi.org/10.1146/annurev.cellbio.23.090506.123237.

Steggerda, S.J., Leijser, L.M., Wiggers-de Bruine, F.T., van der Grond, J., Walther, F.J., van Wezel-Meijler, G., 2009. Cerebellar injury in preterm infants: incidence and findings on US and MR images. Radiology 252 (1), 190–199. https://doi.org/10.1148/radiol.2521081525.

Stoodley, C.J., D'Mello, A.M., Ellegood, J., Jakkamsetti, V., Liu, P., Nebel, M.B., et al., 2017. Altered cerebellar connectivity in autism and cerebellar-mediated rescue of autism-related behaviors in mice. Nat. Neurosci. 20 (12), 1744–1751. https://doi.org/10.1038/s41593-017-0004-1.

Tian, Y., Kolb, R., Hong, J.H., Carroll, J., Li, D., You, J., et al., 2007. TAZ promotes PC2 degradation through a SCFbeta-Trcp E3 ligase complex. Mol. Cell. Biol. 27 (18), 6383–6395. https://doi.org/10.1128/mcb.00254-07.

Tsai, P.T., Hull, C., Chu, Y., Greene-Colozzi, E., Sadowski, A.R., Leech, J.M., et al., 2012. Autistic-like behaviour and cerebellar dysfunction in Purkinje cell Tsc1 mutant mice. Nature 488 (7413), 647–651. https://doi.org/10.1038/nature11310.

Tsai, P.T., Rudolph, S., Guo, C., Ellegood, J., Gibson, J.M., Schaeffer, S.M., et al., 2018. Sensitive periods for cerebellar-mediated autistic-like behaviors. Cell Rep. 25 (2), 357–367. https://doi.org/10.1016/j.celrep.2018.09.039 e354.

Udan, R.S., Kango-Singh, M., Nolo, R., Tao, C., Halder, G., 2003. Hippo promotes proliferation arrest and apoptosis in the Salvador/Warts pathway. Nat. Cell Biol. 5 (10), 914–920. https://doi.org/10.1038/ncb1050.

Wang, K., Degerny, C., Xu, M., Yang, X.J., 2009. YAP, TAZ, and Yorkie: a conserved family of signal-responsive transcriptional coregulators in animal development and human disease. Biochem. Cell Biol. 87 (1), 77–91. https://doi.org/10.1139/o08-114.

Wang, S.S., Kloth, A.D., Badura, A., 2014. The cerebellum, sensitive periods, and autism. Neuron 83 (3), 518–532. https://doi.org/10.1016/j.neuron.2014.07.016.

Watt, K.I., Judson, R., Medlow, P., Reid, K., Kurth, T.B., Burniston, J.G., et al., 2010. Yap is a novel regulator of C2C12 myogenesis. Biochem. Biophys. Res. Commun. 393 (4), 619–624. https://doi.org/10.1016/j.bbrc.2010.02.034.

Wojcinski, A., Lawton, A.K., Bayin, N.S., Lao, Z., Stephen, D.N., Joyner, A.L., 2017. Cerebellar granule cell replenishment postinjury by adaptive reprogramming of Nestin(+) progenitors. Nat. Neurosci. 20 (10), 1361–1370. https://doi.org/10.1038/nn.4621.

Wojcinski, A., Morabito, M., Lawton, A.K., Stephen, D.N., Joyner, A.L., 2019. Genetic deletion of genes in the cerebellar rhombic lip lineage can stimulate compensation through adaptive reprogramming of ventricular zone-derived progenitors. Neural Dev. 14 (1), 4. https://doi.org/10.1186/s13064-019-0128-y.

Wu, S., Huang, J., Dong, J., Pan, D., 2003. Hippo encodes a Ste-20 family protein kinase that restricts cell proliferation and promotes apoptosis in conjunction with salvador and warts. Cell 114 (4), 445–456.

Yui, S., Azzolin, L., Maimets, M., Pedersen, M.T., Fordham, R.P., Hansen, S.L., et al., 2018. YAP/TAZ-Dependent reprogramming of colonic epithelium links ECM remodeling to tissue regeneration. Cell Stem Cell 22 (1), 35–49. https://doi.org/10.1016/j.stem.2017.11.001 e37.

Zhao, B., Li, L., Tumaneng, K., Wang, C.Y., Guan, K.L., 2010. A coordinated phosphorylation by Lats and CK1 regulates YAP stability through SCF(beta-TRCP). Genes Dev. 24 (1), 72–85. https://doi.org/10.1101/gad.1843810.